ORIGIN, DISTRIBUTION, AND RAPID REMOVAL OF HYDROTHERMALLY FORMED CLAY AT MOUNT BAKER, WASHINGTON

GEOLOGICAL SURVEY PROFESSIONAL PAPER 1022-E

Origin, Distribution, and Rapid Removal of Hydrothermally Formed Clay at Mount Baker, Washington

By DAVID FRANK

VOLCANIC ACTIVITY AT MOUNT BAKER, WASHINGTON

GEOLOGICAL SURVEY PROFESSIONAL PAPER 1022-E

A reconnaissance study of the occurrence and geologic implications of clayey volcanic deposits at Mount Baker

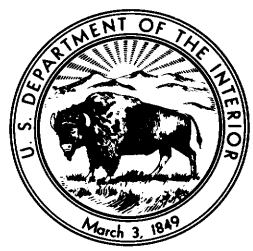

UNITED STATES GOVERNMENT PRINTING OFFICE, WASHINGTON : 1983

UNITED STATES DEPARTMENT OF THE INTERIOR

JAMES G. WATT, *Secretary*

GEOLOGICAL SURVEY

Dallas L. Peck, *Director*

Library of Congress Cataloging in Publication Data
Frank, David
Origin, distribution, and rapid removal of hydrothermally formed clay at Mount Baker, Washington.
(Volcanic activity at Mount Baker, Washington)
(Geological Survey Professional Paper 1022–E)
Bibliography: p. 30
Supt. of Docs. No.: I 19.16:1022–E
1. Clay minerals—Washington (State)—Baker, Mont. I. Title. II. Series. III. Series. Geological Survey Professional Paper 1022–E
QE389.625.F7 553.6'1 81–607131 AACR2

For sale by the Branch of Distribution, U.S. Geological Survey,
604 South Pickett Street, Alexandria, VA 22304

CONTENTS

	Page
Abstract	E1
Introduction	1
Acknowledgments	1
Setting and distribution of alteration	2
Mount Baker	2
Sherman Crater	2
Geology of Sherman Crater	2
Alteration products in Sherman Crater	9
Dorr Fumarole Field	16
Late Quaternary mudflows and avalanches	16
Process of alteration	19
Alteration in crater lake	19
Significance of solution chemistry of alunite	22
Model of near-surface alteration zone	26
Removal of altered debris	26
Hypothetical sources of rapid mass movements	26
Unusually large mass movements	29
Conclusions	30
References cited	30

ILLUSTRATIONS

PLATE	1. Reconnaissance geologic map and cross sections, Sherman Crater	In pocket

		Page
FIGURE	1. Index map of Mount Baker area	E2
	2. Map of the upper cone of Mount Baker	4
	3–7. Photographs of:	
	3. Upper cone of Mount Baker	5
	4. Northwest rim of Sherman Crater	6
	5. Pooch Peak	7
	6. South face of Lahar Lookout	8
	7. Exposures of recent tephras on the south rim of Sherman Crater and at Lahar Lookout	10
	8. Graph showing size distribution of samples of fumarole ejecta and of tephra	12
	9–12. X-ray diffraction patterns of:	
	9. 1975 fumarole ejecta	13
	10. Tephra shb1	14
	11. Tephra shb2	15
	12. Holocene mudflows and avalanche deposits	18
	13. Diagram of the distribution of hydrothermal products	19
	14. Photograph of the crater lake and creek	20
	15. X-ray diffraction patterns of alunitic samples	23
	16. Graph of alunite solubility in acid-sulfate waters	25
	17. Graph of alunite-kaolinite stability	27
	18. Diagram of possible model of alteration zone	28
	19. Diagram of inferred pattern of alteration in Sherman Crater	28
	20. Diagram of hypothetical zones of mass-movement sources	29

TABLES

		Page
TABLE	1. Deposits from eruptions and large mass movements	E3
	2. Minerals in three samples of 1975 fumarole ejecta	12
	3. Minerals in three samples of recent eruptive deposits	15
	4. Minerals in ten samples of Holocene mass movements	17
	5. Chemistry of the crater lake at Sherman Crater	21
	6. Chemistry of the crater creek downstream from crater lake	21
	7. Chemistry of Boulder Creek downstream from crater lake	22
	8. Thermodynamic data for stability calculations of alunite and kaolinite	24

ABBREVIATIONS

a ——activity.
γ ——activity coefficient.
Å ——angstrom.
B.P. ——before the present (expressed in years).
°C ——degrees Celsius.
cm——centimeter.
do ——ditto.
$\Delta G^{\circ}_{f,T}$ ——free energy of formation at standard pressure and specified temperature.
$\Delta G^{\circ}_{r,T}$ ——free energy of reaction at standard pressure and specified temperature.
I ——ionic strength.
K ——kelvin.
kg ——kilogram.
km ——kilometer.
L ——liter.
m ——meter.
m ——molality.
meq ——milliequivalent.
mg ——milligram.
μm ——micrometer.
μmho ——micromho.
mol ——mole.
nd ——not determined.
S°_{T}——entropy at standard pressure and specified temperature.
$\Delta S^{\circ}_{r,T}$ ——entropy change of reaction at standard pressure and specified temperature.
2θ ——in X-ray diffractometry, the angle between the direction of the incident and the diffracted X-ray beam.

ORIGIN, DISTRIBUTION, AND RAPID REMOVAL OF HYDROTHERMALLY FORMED CLAY AT MOUNT BAKER, WASHINGTON

By DAVID FRANK

ABSTRACT

Clay minerals are locally abundant in two hydrothermal areas at Mount Baker—Sherman Crater and the Dorr Fumarole Field. The silt- and clay-size fractions of volcanic debris that is undergoing alteration at and near the ground surface around areas of current fumarolic activity in Sherman Crater are largely dominated by alunite and a silica phase, either opal or cristobalite, but contain some kaolinite and smectite. Correspondingly, the chemistry of solutions at the surface of the crater, as represented by the crater lake, favors the formation of alunite over kaolinite. In contrast, vent-filling debris that was ejected to the surface from fumaroles in 1975 contains more than 20 percent clay-size material in which kaolinite and smectite are dominant. The youngest eruptive deposit (probably 19th century) on the crater rim was also altered prior to ejection and contains as much as 27 percent clay-size material in which kaolinite, smectite, pyrophyllite, and mixed-layer illite-smectite are abundant. The hydrothermal products, kaolinite and alunite, are present in significant amounts in five large Holocene mudflows that originated at the upper cone of Mount Baker. The distribution of kaolinite in crater and valley deposits indicates that, with the passage of time, increasingly greater amounts of this clay mineral have been incorporated into large mass movements from the upper cone. Either erosion has cut into more kaolinitic parts of the core of Sherman Crater, or the amount of kaolinite has increased through time in Sherman Crater.

INTRODUCTION

Clay-rich products of hydrothermal alteration occur in much of the debris in and around vent areas on the upper slopes of Mount Baker, Washington. Similar material is also present at the base of the volcano in some of the deposits that resulted from large mass movements such as mudflows and avalanches.

I undertook this reconnaissance study to assess the possibility that clay-forming processes, particularly hydrothermal alteration, can affect the source, magnitude, and frequency of large volcanic mudflows and avalanches. In studies of other geothermal areas, mineral assemblages resulting from hydrothermal alteration have been interpreted to be the result of metasomatizing fluids from either a deep water source (hypogene alteration) or a surficial source (supergene alteration). Although the direction of heat flow is generally clear in geothermal areas, the origin of the fluids is often ambiguous. Both types of alteration assemblages are considered here to be hydrothermal. Of particular interest are alterations that produce large amounts of kaolinite or smectite by the process of hydrogen metasomatism (Hemley and Jones, 1964).

I examine the geologic setting of two areas in which hydrothermal alteration has taken place at Mount Baker—Sherman Crater and, in less detail, the Dorr Fumarole Field. I then describe the mineralogy and distribution of alteration products in the thermal areas and in the deposits that resulted from mass movements, analyze the solution chemistry that can produce the alteration, and discuss possible ways in which large masses of altered debris can be incorporated into avalanches from thermal areas.

ACKNOWLEDGMENTS

Austin Post, R. M. Krimmel, S. D. Malone, and J. H. Hyde took many of the photographs that were used to prepare the geologic map of Sherman Crater. Hyde also made available split samples of mudflow and avalanche deposits of late Quaternary age. F. C. Ugolini provided facilities for mineral analyses,

primarily by X-ray diffraction, at the pedology laboratory of the University of Washington during 1976 and 1977. In 1975, K. L. Trafton of that laboratory analyzed by X-ray diffraction several samples of material ejected from fumaroles. The University of Washington provided much of the field transportation required for this study during the course of geophysical investigations at Mount Baker in 1975 and 1976 by S. D. Malone of the Geophysics Program. He, Post, Al Rohay, Alex Horstman, and Alex Bittenbinder also kindly helped collect water samples from Sherman Crater. I am grateful to G. C. Bortleson, D. R. Crandell, P. L. Heller, D. A. Johnston, D. R. Pevear, Robert Schoen, and D. A. Swanson for their critical comments on this report.

SETTING AND DISTRIBUTION OF ALTERATION

MOUNT BAKER

Mount Baker is a calc-alkaline andesitic stratovolcano 48 km inland near the northern end of the Cascade Range in northwest Washington (fig. 1). The present cone began to grow during the Pleistocene (Coombs, 1939, p. 1500), but it is presumed to be no older than lava flows northeast of Mount Baker for which two potassium-argon dates of about 400,000 years B. P. (before present) were reported by Easterbrook and Rahm (1970, p. 20). The present cone is also younger than the Black Buttes, a greatly eroded but as yet undated eruptive center on the west flank of Mount Baker (Coombs, 1939, p. 1500). Recent petrographic studies (Swan, 1978) indicate that a wide range of volcanic rock types from basalt to rhyolite occurs in all these areas, although andesite and dacite predominate in most of Mount Baker proper.

Hyde and Crandell (1978) examined volcanic deposits of late Quaternary age on the lower slopes of Mount Baker, and their data are summarized in table 1. Deposits that have been recognized record several events since the Fraser Glaciation, including three eruptive periods of tephra and one of pyroclastic flows and lava from a central vent, and one eruptive period of tephra and lava from a flank vent at Schriebers Meadow (fig. 1). Additionally, large mudflows and avalanches occurred at least eight times during this period. Clast lithology, large volume, and long travel path indicate that most of the mudflows originated from high on the volcano (Hyde and Crandell, 1978). Exceptions are the youngest mudflow in the Middle Fork Nooksack River valley and the Rainbow Creek avalanche which they thought probably originated at cliffs on the upper valley walls (Hyde and Crandell, 1978, p. 9, 10).

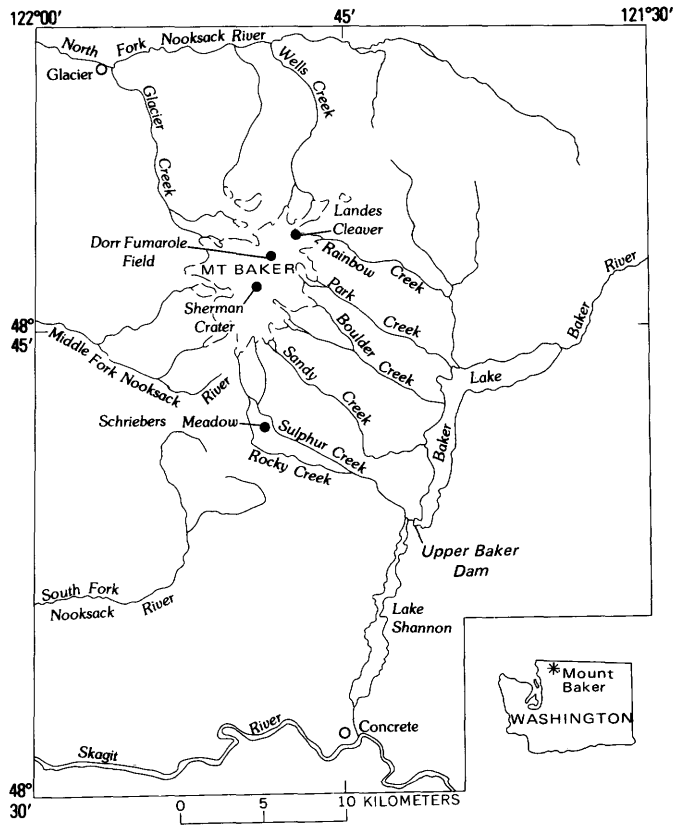

FIGURE 1.—Mount Baker area, Washington. Base is revised from U.S. Geological Survey, North Cascades, scale 1:250,000.

More recently, much smaller debris avalanches have fallen from the rim of Sherman Crater at least eight times during the last two decades (Frank and others, 1975). The latest volcanic event of significance at Mount Baker consisted of a sharp increase in thermal activity in Sherman Crater during 1975 (Malone and Frank, 1975; Eichelberger and others, 1976; Frank and others, 1977; Friedman and Frank, 1980). Thermal activity decreased somewhat after 1975, but to date (November 1981) persists at a level of activity greater than that prior to 1975 (Krimmel and Frank, 1980).

SHERMAN CRATER

GEOLOGY OF SHERMAN CRATER

Sherman Crater is a steep-walled basin about 600 m in diameter, centered about 800 m south of and 400 m lower than the summit of Mount Baker (figs. 1, 2). The crater is partly filled by a glacier that descends southward from the summit area. Rock exposures that represent remnants of the Sherman Crater rim are Lahar Lookout on the east, Sherman Peak on the

TABLE 1.—*Deposits at lower elevations from eruptions and large mass movements at Mount Baker, summarized from Hyde and Crandell (1978)*

[nd, not determined; B.P., before present]

Eruptive deposit[1]	Approximate age (years)	Source	Probable distance traveled (km)	Estimated volume of deposit ($\times 10^6 m^3$)
Tephra, shb1	Last few hundred years	Sherman Crater	>10	nd
Tephra, shb2 (?)[2]	500–6,000 B.P.	Mount Baker	>10	100–200
Lava flow and tephra	6,600–10,400 B.P.[4]	Schriebers Meadow	12 (flow)	nd
Several pyroclastic flows and two lava flows shb3 (?)[2].	8,700 B.P. (?)[3]	Sherman Crater	>11	340–380 (also includes several mudflows.)
Tephra	10,400 B.P.[4]	Mount Baker	>10	nd

Mass-movement deposit	Approximate age (years)	Location	Distance traveled (km)	Volume
Eight debris avalanches.	A.D. 1958–79	Boulder Glacier	3	0.035 each.
Mudflow	Last few hundred years	Boulder Creek	11	nd
Rock avalanches	——do——	Rainbow Creek	>9	13
Mudflow	——do——	Boulder Creek	11	nd
Mudflow	500–600 B.P.	Park Creek	14	1–2
Mudflow or avalanche.	300–6,000 B.P.	Middle Fork Nooksack River.	8	1
Mudflow	6,000 B.P.	Middle Fork Nooksack River.	>29	40–50
Do.	6,000 B.P. (?)	Sulphur Creek	>12	nd
Do.	6,000 B.P. (?)	Baker Pass	nd	nd
Mudflow	6,200–6,600 B.P.[4]	Park Creek	14	27
Several mudflows interbedded with pyroclastic flows.	8,700 B.P. (?)[3]	Boulder Creek	>11	(Volume included above with eruptive deposits.)
Mudflow	6,600–10,400 B.P.[4]	Sulphur Creek	>12	nd
Mudflow	>10,400 B.P.[4]	——do——	>6	nd

[1]Abbreviations refer to the designations of deposits used in this report.
[2]Tentative correlation between crater and valley deposits.
[3]Questionable date (Hyde and Crandell, 1978, p. 4).
[4]Age rounded from that listed by Hyde and Crandell (1978, table 1).

southeast, and Pooch Peak[1] on the southwest. Two low points on the rim are a 60-m-deep saddle on the west and a 200-m breach on the east. All surface drainage in Sherman Crater flows through the east breach.

I conducted about 10 days of field reconnaissance during 1975 and 1976 and used aerial photographs to construct a geologic map and cross sections (pl. 1) of Sherman Crater. Petrologic names are not used extensively in this report because most rocks are not what they once were, owing to hydrothermal alteration. Rocks are divided into two types of units: (1) lava flows, brecciated lava flows, or sills, and (2) pyroclastic breccias or tephra. The units originated from two different eruptive centers, one near the summit and one at Sherman Crater. The October 1976 pattern of anomalously warm ground (thermal area) was mapped by utilizing field observations and by discriminating unusually steep snow margins in aerial photographs (Frank and Post, 1976). Locations of the larger fumaroles are noted within the thermal area (pl. 1).

Rocks that form the bulk of the upper part of Mount Baker, particularly in the northwest to northeast sector, were erupted from a vent near the summit. A portion of a crater rim that was exposed in 1940, but that is now ice-covered, prompted the designation of Summit Crater for the ice-covered summit plateau (Frank and others, 1975, p. 77). The Summit Crater is poorly defined and is probably nested within, or is marginal to, a larger crater which includes much of the southeast-facing cirque between the summit and Sherman Crater (fig. 2). Volcanic deposits originating from near the summit can be distinguished from those from Sher-

[1]The southwest rim of Sherman Crater is not named on published maps. For convenience of reference in this report, the rock mass is called Pooch Peak, the name that has been commonly used during the last 7 years by those involved in monitoring Mount Baker.

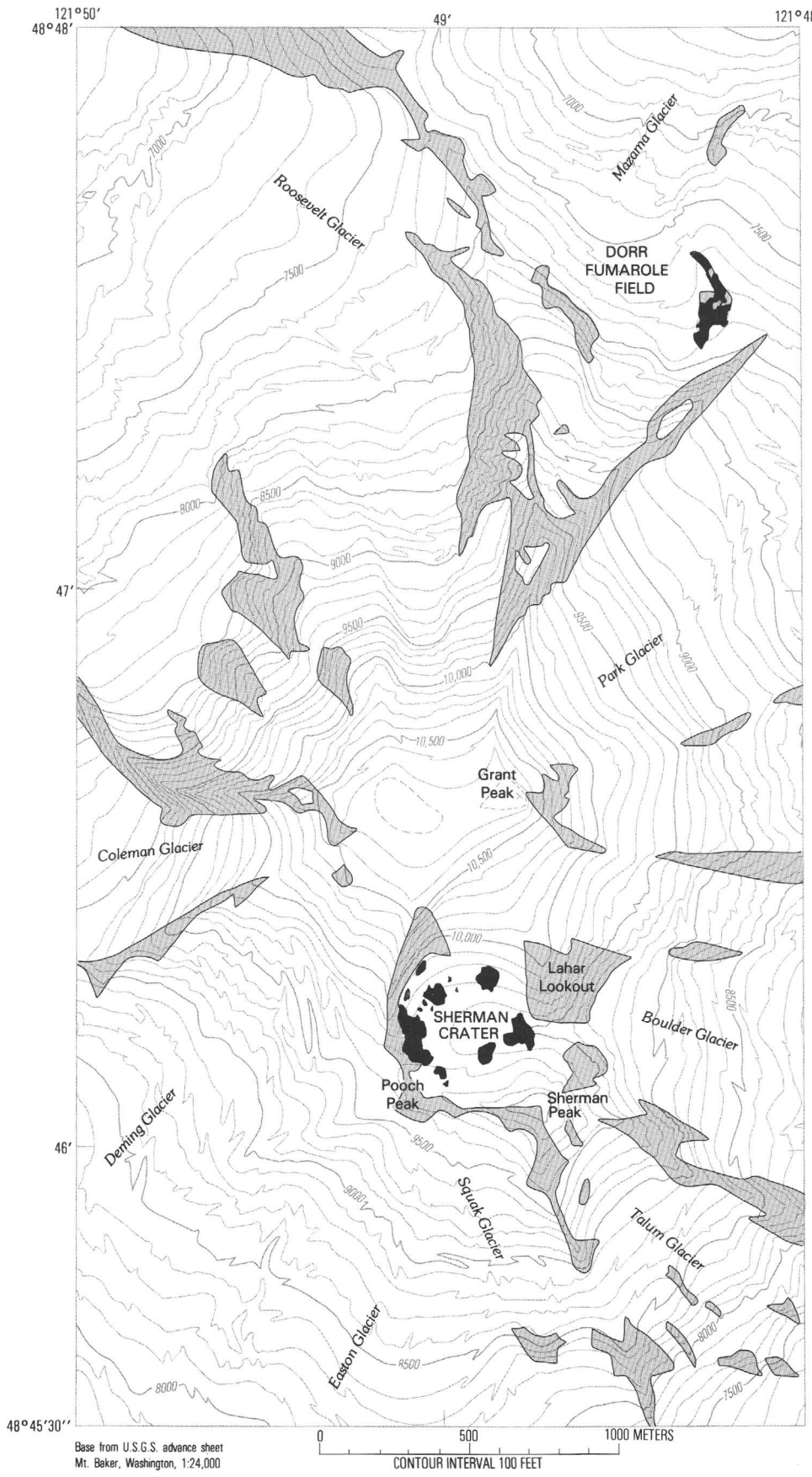

FIGURE 2.—Upper part of the cone of Mount Baker, Washington. Two thermal areas (solid black) are Sherman Crater and the Dorr Fumarole Field. Rock outcrops are shown by light stipple. Map is modified from Friedman and Frank (1980).

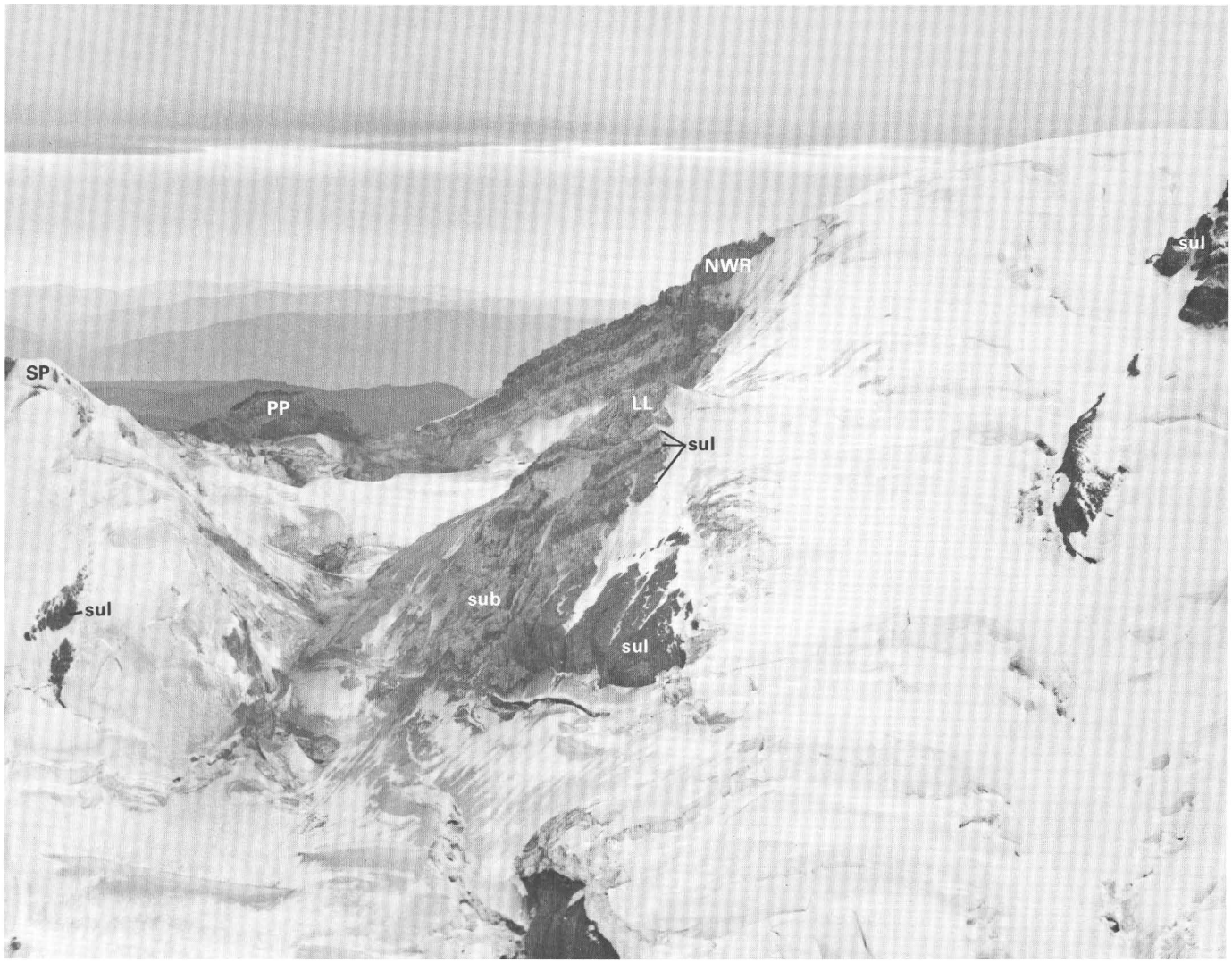

FIGURE 3.—The upper part of the cone of Mount Baker, September 13, 1976. In this view looking to the west, Sherman Crater lies between Sherman Peak (SP) and the summit (upper right). Lava flows or sills (sul) and pyroclastic breccias (sub) erupted from near the summit form the middle and lower right of the east face of Lahar Lookout (LL), the lower part of Sherman Peak, and the northwest rim (NWR) of Sherman Crater. Rocks erupted from Sherman Crater cap and form the ventward faces of Sherman Peak and Lahar Lookout, and form all of Pooch Peak (PP).

man Crater primarily by strike and dip. At Sherman Crater, rocks erupted from vents in the summit area are referred to here as the summit sequence (sul and sub on pl. 1). They form the lower part of the east side of Lahar Lookout, the lower part of Sherman Peak, and the northwest rim of Sherman Crater (pl. 1). Rocks erupted from a vent at Sherman Crater (shl and shb) include the upper part and west of Lahar Lookout, the upper part of Sherman Peak, the south and west rims of Sherman Crater, and Pooch Peak.

The east face of Lahar Lookout (fig. 3) provides a good exposure of the summit sequence in which units dip southeastward away from the summit area. At the bottom of this exposure, the northeast base of Lahar Lookout contains a massive flow or sill which aerial photography shows to be distinctively riddled with light-colored, more resistant veins as much as 1 m wide. Overlying material includes a thick section of pyroclastic breccias and three lava flows each less than 15 m thick.

A spectacular exposure of the summit sequence forms the steep northwest rim of Sherman Crater (fig. 4). On this wall, a section across the rim of a summit vent (arrow in fig. 4) occurs where vent-filling material lies toward the east. The wall is dominated by units as much as 30 m thick, which include five lava flows or sills and a prominent white pyroclastic breccia.

The summit sequence of eruptions was followed by

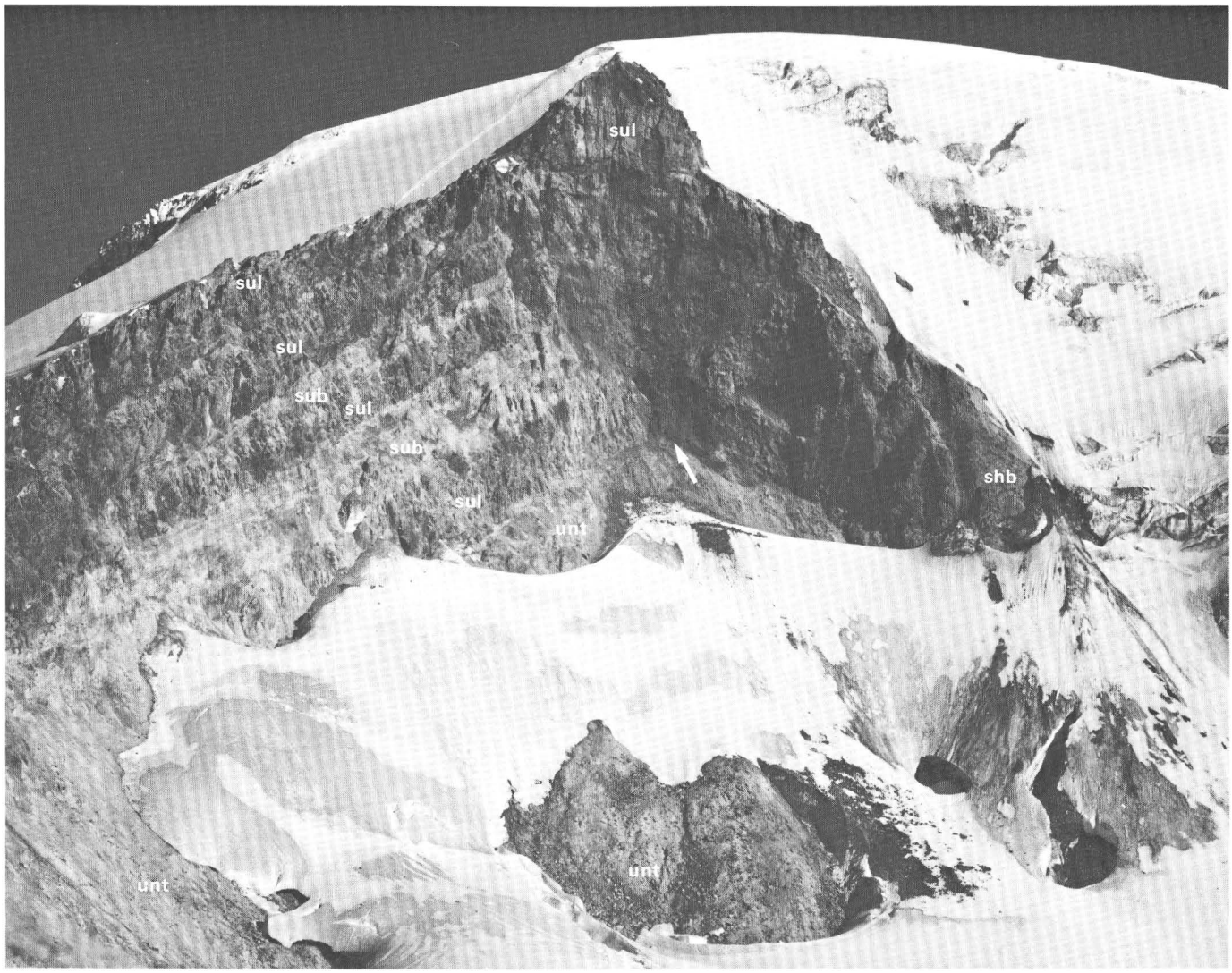

FIGURE 4.—Northwest rim of Sherman Crater as seen from the south rim on August 31, 1976. This wall of Sherman Crater exposes a 120-m-thick section of lava flows or sills (sul) and pyroclastic breccias (sub) erupted from a vent near the summit. The sectioned rim (arrow) of this vent separates the thicker, flat-lying or east-dipping units on the vent side (to the right) from the southwest-dipping units on the left. Rocks from Sherman Crater thinly cap the top of the rim and probably form the far right margin of the exposure (shb). Clusters of active fumaroles (unt) have melted ice pits within the crater glacier.

eruptions from the present site of Sherman Crater. An early phase of these eruptions built lava and pyroclastic debris up to at least the present height of Sherman Peak. At Sherman Peak, more than 100 m of gently south-dipping breccias overlie more steeply dipping lava flows from the summit. Pryoclastic breccias from Sherman Crater also extend along the south rim to Pooch Peak. At Pooch Peak, a thick unit of breccias overlies three thin (<15-m-thick) lava flows (fig. 5). The ventward side of Pooch Peak is particularly well indurated and forms a slightly overhanging wall more than 60 m high. The breccia contains blocks as much as 1 m across of brown to gray porphyritic lava and red scoria in a white to light-gray or tan tuffaceous matrix.

Additional products of the early eruptions from Sherman Crater make up part of the west half of Lahar Lookout. A section through the Sherman Crater rim (fig. 6) is beautifully exposed on the south side of Lahar Lookout where west-dipping breccias and three thin (<10-m-thick) lava flows or sills bank along a sharp, unconformable contact against southeast-dipping deposits erupted from the summit area. The crater fill is topped by a massive west-dipping breccia at least 30 m thick. Remnants of a similar vent-filling breccia occur on the east edge of the northwest rim (fig. 4) and likely form most of the steep, ice-covered north rim of Sherman Crater (pl. 1).

The early eruptions at Sherman Crater were followed

FIGURE 5.—Pooch Peak as viewed from the west rim of Sherman Crater on August 8, 1975. Three lava flows (shl) along the outward base of Pooch Peak are nearly flat lying on the left and begin to dip as much as 10° southwest toward the right. The overlying pyroclastic unit (shb) is more than 60 m thick. The west rim in the foreground is blanketed by the two recent tephras, shb2 and shb1. The surface and first subsurface (arrow) layers of debris in the snow are mostly 1975 fumarole ejecta. Other layers form annually and are rock dust blown off the crater rim. A group of three packs (circle) on the snow surface outside the crater at lower right shows scale.

or were accompanied by massive removal of much of the material on both the east and west sides of the crater between Sherman Peak and the summit area. The material that was removed comprised rocks of the summit sequence as well as products of Sherman Crater. After material was removed from the east side and an east breach was opened, eruptions deposited a fill at least 90 m thick of breccias (shb3, pl. 1) in the breach. Erosion, or explosions, have subsequently cut through much of this fill. Although rock-slide debris and tephra cover most of the surface and exposures are poor (fig. 6), the few breccia units that protrude through the cover are almost flat lying in the breach and dip gently eastward outside the breach. These relationships indicate that the fill was deposited after the breach was opened.

Inasmuch as the east breach fill is the youngest relatively large pyroclastic deposit in Sherman Crater, it and possibly much of the missing material from the east rim are tentatively correlated with the 8,700(?)-year-old Boulder Creek assemblage (table 1). This assemblage includes the youngest pyroclastic-flowage deposits of large volume at the base of the cone (Hyde and Crandell, 1978). By similar reasoning, the removal of material from the south and west rims might account, at least in part, for the large 6,000-year-old mudflow in the Middle Fork Nooksack River valley (table 1).


shb1
sul
shb
sul
shl
sub
shb
sul
sub
un
shb3

These removal events left a topography on the south and west rims similar to that of the present; the next-to-youngest deposit (shb2) was subsequently erupted. This deposit is a weakly indurated tephra with a highly altered, clayey top. The interior consists of dark-gray to black porphyritic clasts of andesitic lapilli in a light- to dark-gray tuffaceous matrix (fig. 7*A*). Clasts contain a brown to tan rind near the surface of the deposit, and the matrix has a brown to red tinge. This deposit blankets much of the crater rim and possibly makes up a large part of the undifferentiated surficial debris (un) on plate 1. The thickness of the tephra is estimated to be at least 1 m on the south and west rims. On the basis of stratigraphic position, the unit is tentatively correlated with the 500- to 6,000-year-old tephra (table 1) found at the base of Mount Baker. A mineralogical correlation could not be made because of extensive alteration of the crater deposits.

The youngest eruptive deposit (shb1) on the rim of Sherman Crater is a white tephra that contains abundant white to light-gray and sparse black lapilli, as much as 10 cm in diameter, in a white to tan, clayey matrix (fig. 7). A 50-cm-thick remnant of this tephra caps Lahar Lookout (fig. 7*B*). It is almost continuous along the south rim to Sherman Peak where it is at least 50 cm thick. The deposit occurs along the west rim and lightly dusts the top of Pooch Peak and the northwest rim. Thin swaths can also be seen on the lower southeast ridge of Sherman Peak, upper Boulder Ridge, and the east face of the summit. Unit shb1 is mineralogically distinctive and is correlated with the young white lithic tephra found at the base of Mount Baker (table 1).

The white tephra is conspicuously truncated by erosion along a 40-m stretch of the middle part of the south rim of Sherman Crater and on the east face of Lahar Lookout. Debris avalanches have probably occurred from these areas since deposition of the unit. Similar debris avalanches (table 1) have been observed to recur every 2–4 years during the last 20 years from the north face of Sherman Peak.

◀ FIGURE 6 (facing page).—South face of Lahar Lookout as seen from Sherman Peak on August 17, 1974. Lahar Lookout contains rock erupted both from near the summit and from Sherman Crater. Arrow points out the unconformable contact between a thick, light-colored, west-dipping tuff-breccia (shb) from Sherman Crater and southeast-dipping lava flows (sul) and breccias (sub) of the summit sequence. The tuff-breccia is overlain by three thin lava flows (shl) and a thick, well-indurated pyroclastic breccia. A remnant of a thin tephra (shb1) caps Lahar Lookout. At the east breach (foreground), remnants of a pyroclastic fill (shb3) that originated from Sherman Crater protrude through undifferentiated surficial material (un) made up mostly of rock-slide debris.

The most recent air-fall deposit in Sherman Crater can no longer be recognized as an individual unit except where it has been temporarily incorporated into firn. This deposit is the fumarole ejecta that accompanied the 1975 increase in thermal activity, and probably was produced continuously from March to September 1975 (Frank and others, 1977, p. 8). The ejecta comprise about 1000 m^3 of fine-grained, clayey dust and mud of nonmagmatic origin deposited in a thin (≤ 1 cm) swath across Sherman Crater and a few hundred meters outside the crater.

The time periods between and during most of the eruptive episodes represented by deposits at Sherman Crater are unknown. The relatively large volumes of remnants of the earlier activity suggest that these eruptions possibly constituted the final phase of Pleistocene volcanism that built most of the south side of Mount Baker. Conceivably, however, not only the east breach fill (shb3) but also many other pyroclastic breccias in Sherman Crater are all part of the same eruptive episode that produced the Boulder Creek assemblage 8,700(?) years ago. This hypothesis seems unlikely at present because of the lack of recognized Holocene pyroclastic flows and lava flows from Sherman Crater in valleys other than Boulder Creek.

ALTERATION PRODUCTS IN SHERMAN CRATER

Coombs (1939, p. 1500) first recognized the large amount of opaline and sulfurous alteration products in Sherman Crater. Subsequently, Bockheim and Ballard (1975) identified both montmorillonite and kaolinite in surficial debris collected from the west rim and near the east breach. In the present study, I attempted to determine the alteration products that are indicative of current hydrothermal activity at the surface near fumaroles and of current and past activity at some depth below the surface as represented by eruptive products and fumarole ejecta that were altered prior to emission.

Mineral analyses were made primarily by X-ray diffraction (XRD) with a Picker-Nuclear[2] diffractometer and nickel-filtered Cu$K\alpha$ radiation. Most of the XRD traces were recorded at a rate of 2° of 2θ per minute. The vertical-scale range varies in subsequent illustrations of XRD patterns and should be noted when comparing different traces. For example, a given XRD peak height on a trace recorded at a scale range of 1000 would represent 3.3 times the amount of XRD geiger counts per second as the same peak height at a scale

[2]Use of trade names in this report is for descriptive purposes only and does not constitute endorsement by the U.S. Geological Survey.

range of 300. In subsequent tables, the notations M, X, and T for major, minor, and trace diffraction peaks were made on the basis of XRD peak height. Such an analysis provides a qualitative basis for estimating the relative abundance of minerals.

About 60 samples of unconsolidated debris analyzed for this study were split by wet-sieving at 50 μm and then X-rayed, either as oriented mounts on glass slides or as unoriented powders in standard aluminum boxes. Clay samples provided by J. H. Hyde had been separated by gravity-settling methods. Additional key samples of material from Sherman Crater were split into size fractions by the Kittrick and Hope (1963) method, which consists of centrifuging the samples after removal of soluble salts and free iron oxides.

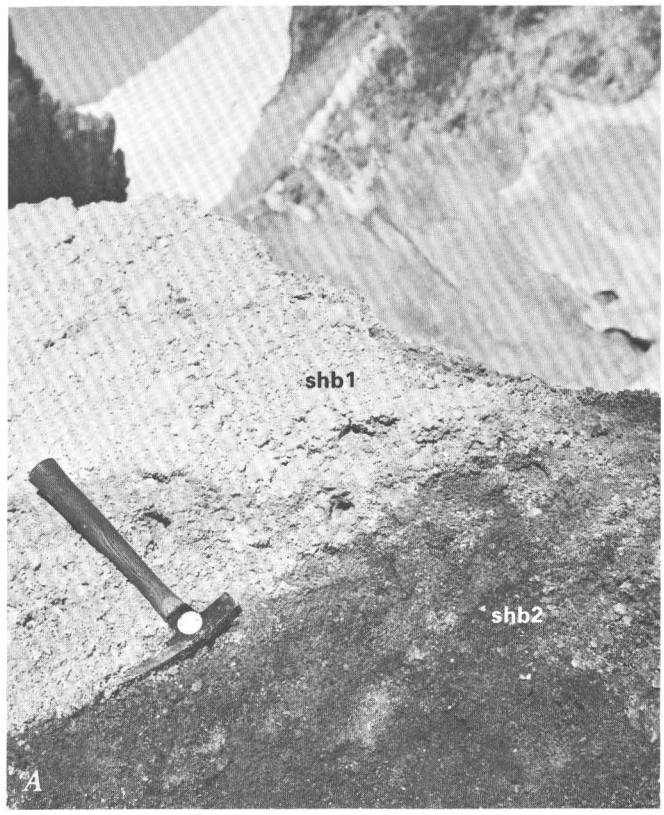

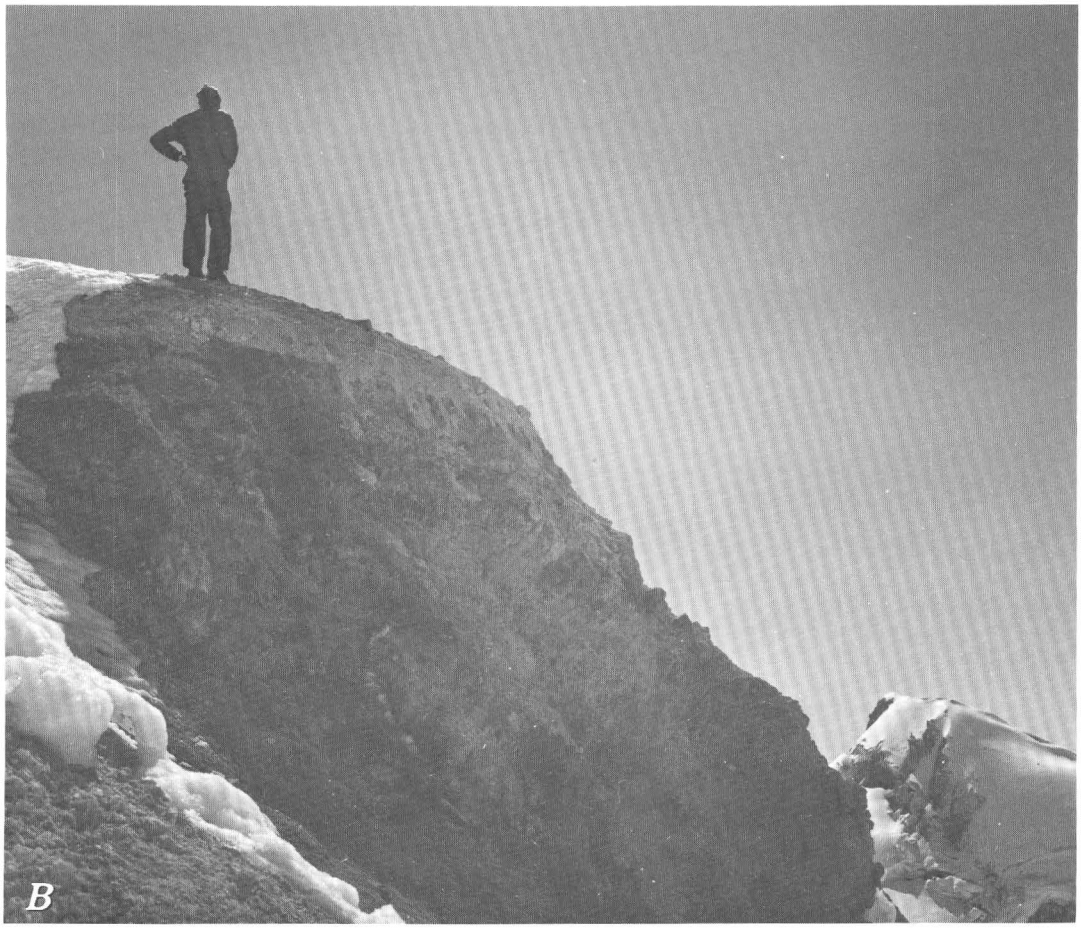

FIGURE 7.—Exposures of recent pyroclastic breccias. *A*, Two most recent tephras (shb2 and shb1) in an excavation in south rim of Sherman Crater on August 31, 1976. Head of pick lies along contact. Lighter color of upper unit at the ground surface results from air-drying. This locality is site for samples Bd-26-1 and Bd-26-2. *B*, Natural exposure of recent white tephra (shb1) at crest of Lahar Lookout, September 13, 1977. Sherman Peak in background.

Organic material was not removed. Fractions less than 5 μm were saturated with K^{+1} and Mg^{+2} and equal weights were sedimented onto glass slides for XRD analysis. Glycolation and heat treatments were used for determination of clay minerals. Mineral identification was made by criteria described by Brown (1961) and Carroll (1970).

Kaolinite, as used here, refers to the kaolinite group of minerals, because no discrimination was made between dickite, metahalloysite, and kaolinite proper. Hydrated halloysite, however, which is a more easily distinguishable member of the kaolinite group, was not detected in any samples. The term smectite is used here in the general sense for that group of minerals, including montmorillonite, whose lattice *c*-dimension expands to about 17Å after glycolation. No further analysis was made to differentiate between various types of smectite.

The terminology for silica minerals other than quartz is based on the degree of disorder in the cristobalite peaks. Samples that display well-ordered α-cristobalite with only a small degree of line broadening and accompanied by tridymite are tabulated as containing α-cristobalite and tridymite. Samples that show disordered cristobalite accompanied by tridymite are tabulated as containing opal-CT. In some samples, a broad hump at about 4.1Å in place of a distinct cristobalite peak suggests the presence of amorphous opal, but because of poor discrimination of the hump and masking by other mineral peaks, this phase is not tabulated. These three types of XRD patterns represent respectively, opal-C, opal-CT, and opal-A in the nomenclature of Jones and Segnit (1971, p. 57–59).

The copper radiation used in this study is relatively less sensitive for iron-bearing minerals (Carroll, 1970, p. 46–47). This lower sensitivity is particularly apparent in the detection of moderately abundant pyrite and magnetite in many samples. The determined abundance of such minerals is therefore underrepresented. Futhermore, the main magnetite peak is often masked by peaks of other minerals, so that although possibly present, magnetite is not tabulated.

Hydrothermal alteration accompanies the thermal activity now occurring in Sherman Crater. In general, the thermal activity (Frank and others, 1977) consists of clusters of sulfurous fumaroles surrounded by large areas of warm ground. Fumarole temperatures are commonly near the boiling point of water for the crater altitude (≈90°C), although temperatures as high as 131°C developed near the east breach in 1975 (Malone, 1979, p. 245), and at least 96°C on the west rim in 1976. Plate 1 shows 28,500 m^2 of snow-free thermal ground in October 1976, or about 17 percent of the crater area.

An attempt was made to find a systematic pattern of alteration in surficial debris at various distances from fumaroles or within different temperature zones. Several samples from the west rim were collected from an area where surface temperatures spanned a 30°C range within 15 m from a fumarole cluster. Temperatures were delineated with a ground-based thermal infrared scanner sensitive to 8–14 μm radiation.

Silt and clay fractions of these samples contain a suite of minerals that vary somewhat in proportion, but no distinct zonation of mineral assemblages was observed. The samples contain primarily cristobalite, quartz, alunite, sulfur, and pyrite with lesser amounts of kaolinite, tridymite, jarosite, and gypsum. In most samples, alunite is the dominant mineral in the X-ray patterns of both oriented and random mounts. These samples were all within the thermal area of the west rim.

An analysis of alteration products presently at depth within the fumarole system was facilitated in 1975 by the fumarole ejecta that accompanied the opening of new fumaroles. Most of the ejecta came from one large fumarole (the new main fumarole of Frank and others, 1977, p. 8) and thus represents a sampling of alteration products formed at some depth beneath this locality at the southwest base of Lahar Lookout (pl. 1).

Babcock and Wilcox (1977) examined the coarse-grained fractions (>10 μm) of several samples of fumarole ejecta and found them to be generally dominated by a silica phase (opal, tridymite, or cristobalite), pyrite, and scoria or lithic fragments, with lesser sulfur, pyroxene, magnetite, feldspar, gypsum, alunite, anhydrite, and glass. I examined several size fractions of some of these samples (table 2); the results are in general agreement with those of Babcock and Wilcox (1977), but with more discrimination of the finer components.

Three samples of fumarole ejecta contain 20–27 percent of clay-size material (fig. 8). XRD analysis (table 2) shows that kaolinite and smectite dominate the clay fractions (<2 μm) and α-cristobalite, alunite, and, to a lesser extent kaolinite, dominate the silt fractions (2–50 μm). Lesser components in these sizes are mixed-layer illite-smectite, illite, pyrophyllite, tridymite, opal-CT, quartz, gypsum, sulfur, and feldspar. A representative example of the XRD patterns and mineral identifications is shown in figure 9. The samples in table 2 span the time of ejecta production from the early part of the increased activity, March 1975 (Bd-2-2), to the latest period that new ejecta was observed, September 1975 (Bm-1-1). Three of the samples in table 2 are air-fall material and the fourth (Bm-1-1) is mud that flowed over the fumarole lip. No change through time is apparent in the fine-grained components of these samples, although Babcock and Wilcox (1977, p. 25) found that pyrite decreased in the coarser fractions.

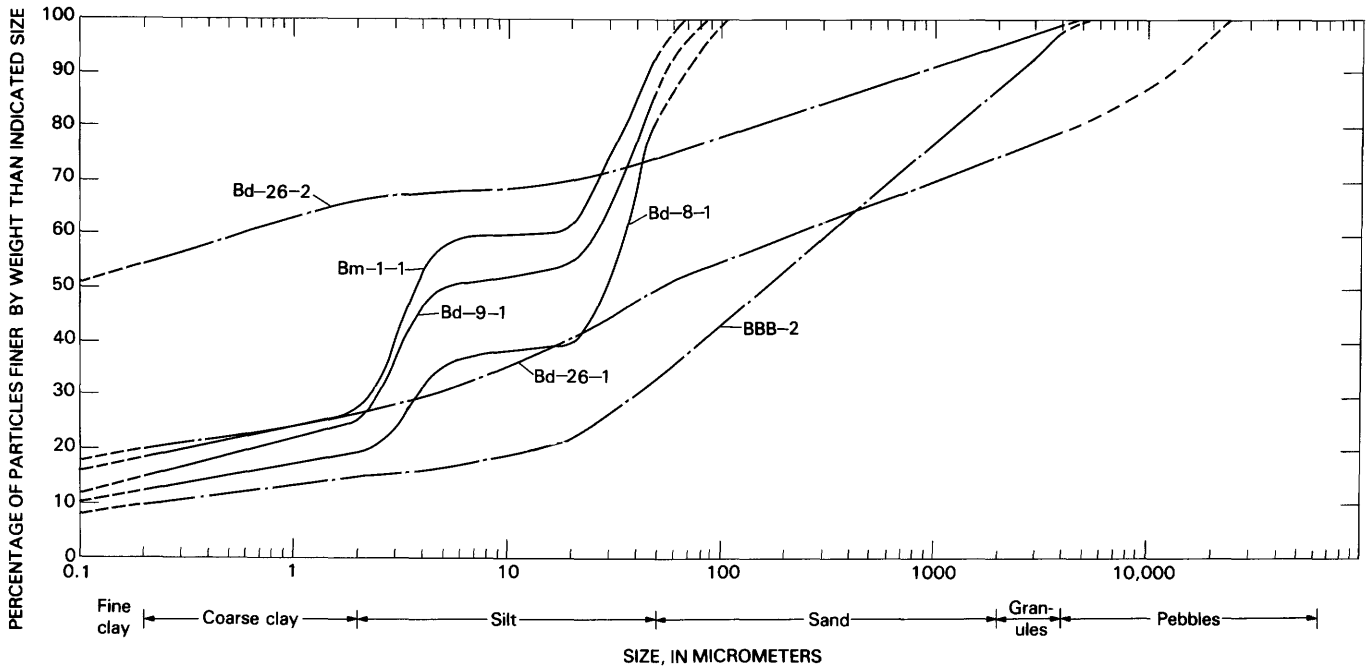

FIGURE 8.—Size distribution of three samples of 1975 fumarole ejecta (Bd-8-1, Bd-9-1, Bm-1-1), two samples of tephra shb1 (Bd-26-1, BBB-2), and one sample of tephra shb2 (Bd-26-2). Sample localities are shown on plate 1, except for BBB-2 which is from Landes Cleaver (fig. 1).

TABLE 2.—*Minerals identified by X-ray diffraction analysis of 1975 fumarole ejecta from Sherman Crater*

[M, X, T: major, minor, and trace diffraction peaks, respectively]

Size fraction, in micrometers (μm)	Smectite	Mixed-layer illite-smectite	Illite	Chlorite	Pyrophyllite	Kaolinite	Alunite	Quartz	Tridymite	α-Cristobalite	Opal-CT	Feldspar	Gypsum	Sulfur	Pyrite
Sample No. Bd-2-2, ejected Mar. 10–May 14, 1975															
50–2000						T	X	T	T	X	X	T		T	T
5–50	T	T	T			X	M	T	X	M		T		T	
2–5	M	T	T		T	M	T	T	T	X	T	T		T	
0.2–2	M		T		T	M									
<0.2															
Sample No. Bd-8-1, ejected Mar. 10–June 11, 1975															
50–2000	T	T				T	X	T	X	M	T			T	T
5–50	T				T	X	M	X	X	M			X	T	X
2–5	T	T	T		T	M	X	T	T	X	T	T		T	
0.2–2	M		T			M	T							T	
<0.2	M		T			M									
Sample No. Bd-9-1, ejected June 14–30, 1975															
50–2000	T	T				T	X	T	T	X	T			X	T
5–50	T	T				T	M	T	X	M		T		T	
2–5	T	T		T	T	X	T	T	T	X	T	T		T	
0.2–2	M	T	T		T	M									
<0.2	M					M									
Sample No. Bm-1-1, ejected Sept. 19, 1975															
50–2000	T				T	T	X	T	T	M			M	X	T
5–50	T	T				X	M	T	T	M		T			T
2–5	T		T		T	X	T	T	T	X	T			T	
0.2–2	M	T		T	T	X									
<0.2	M	T			T	M									

An older assemblage of alteration products is present in the white tephra (shb1) on the crater rim. This deposit was sampled from localities on Lahar Lookout, Sherman Peak, the south and west rims of Sherman Crater, and near the summit of Mount Baker. A size analysis of the matrix indicates a clay fraction of 27 percent for the sample from the south rim (fig. 8). The silt and clay fractions contain a suite of minerals similar to the 1975 fumarole ejecta (table 3; fig. 10). Differences include much more microcrystalline quartz, more smectite, pyrophyllite, illite, regular mixed-layer illite-smectite, and jarosite, and less or no sulfur and pyrite. Fine-grained clasts in the tephra include hard, dark-gray fragments primarily of quartz and smectite; hard, white fragments of microcrystalline quartz that resembled chert in hand specimen; and soft, white fragments of opal-CT, alunite, and gypsum. This tephra also contains a few clasts that display textural features suggestive of porphyritic andesite with opal in feldspar pseudomorphs, gypsum and opal in the groundmass, and alunite in a fine meshwork of veins. Several clasts contain gypsum coatings, veins, and vesicle fillings.

The white tephra (shb1) is correlated on the basis of field appearance, stratigraphic position, and mineralogy with the distinctive white tephra found at the base of the volcano (table 1). A sample of this tephra was collected from Landes Cleaver, 4 km northeast of

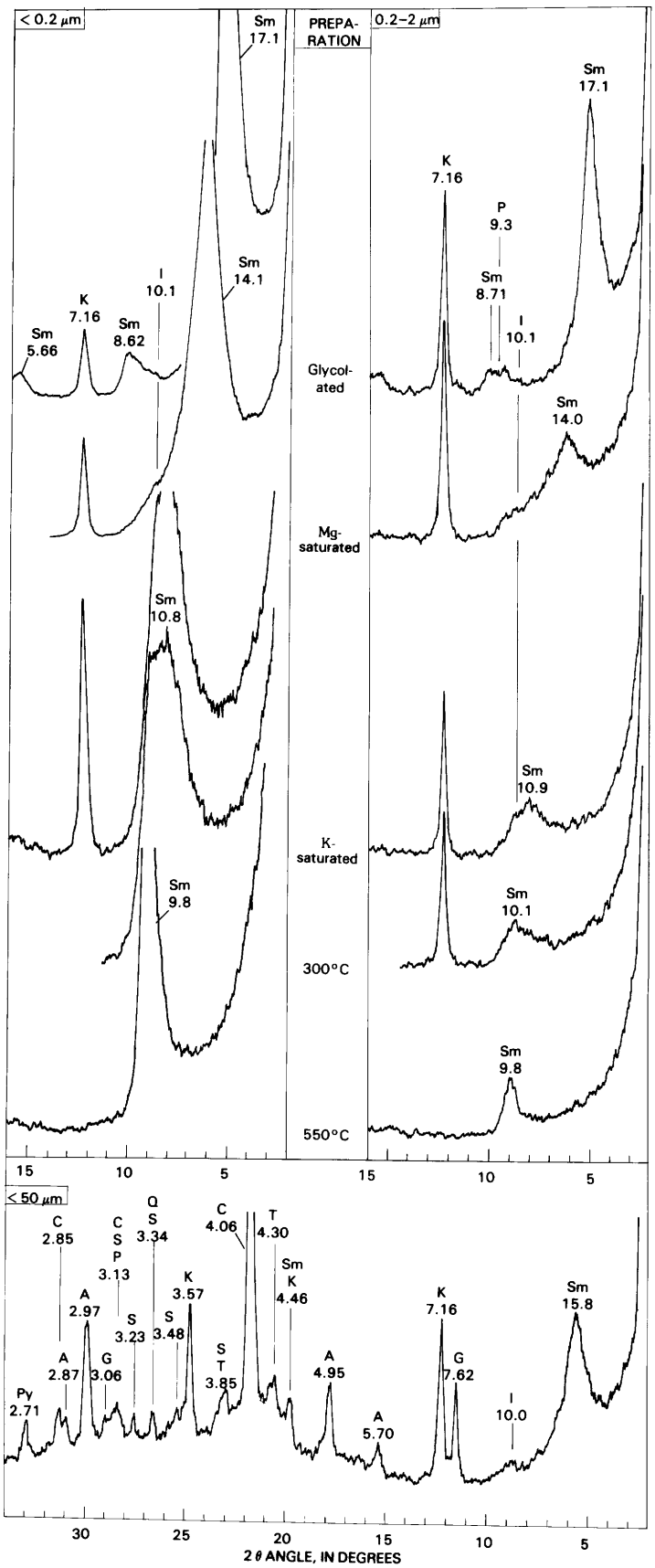

Sherman Crater (fig. 1). This sample (BBB–2) contained 15 percent clay-size material (fig. 8), and it is much better sorted than the tephra in the crater. Both samples contain the same suite of minerals and only a small amount of glass (table 3). The mineralogy suggests that the tephra was derived from vent-filling debris that underwent extreme hydrothermal alteration to an assemblage of silica, alunite, kaolinite, and other clays at some time prior to eruption. As discussed later, this mineral assemblage should not result from Holocene weathering in the type of alpine environment that occurs on the lower slopes of Mount Baker.

The next oldest deposit on the crater rim is the gray to brown tephra (Shb2). This unit was sampled from localities on the south rim (fig. 7*A*) and on the west rim. The tephra is highly altered near the surface, in places to a deep red. It grades into a less altered, more indurated material within less than 50 cm from the surface. In the more highly altered zone, dark-gray friable clots that in outcrop appear to be pseudomorphic after vesicular andesitic lapilli are shown by XRD analysis to be primarily feldspar and smectite accompanied, in some cases, by gypsum (table 3). A sample of the once-ashy matrix contains 67 percent clay-size material (fig. 8). XRD analysis of the clay fraction detected only smectite and a small amount of kaolinite (fig. 11). The remainder of the matrix contains primarily smectite, feldspar, and gypsum, with lesser opal-CT, jarosite, kaolinite, and sulfur. Typically striking on the surface of this unit are large gypsum crystals as much as 1 cm long that have a selenite habit. The gypsum appears to have formed after deposition of the unit. The large crystals are particularly abundant along the south rim where, with proper sun angle, they produce a shimmering glitter on the ground surface.

Significant hydrothermal alteration of this tephra

FIGURE 9.—X-ray diffraction (XRD) patterns of a sample of fumarole ejecta (Bd–8–1) collected from the snow surface in Sherman Crater and representing material emitted during March–June 1975. Size separates of <50, 0.2–2, and <0.2 μm are shown. Silt and clay (<50 μm) pattern is from an unoriented mount in an aluminum box. Clay patterns are from oriented mounts of 90 mg each on glass slides. Pretreatment preparations for clay fractions include saturation with K^{+1} and subsequent heating for 1 hour each at 150° (not shown), 300°, and 550°C, and saturation with Mg^{+2} and subsequent glycolation. XRD peaks are noted with the interplanar "*D*" spacings for Cu*K*α radiation listed in angstrom units (Å). Vertical-scale range is 1000 for patterns of <0.2 μm Mg-saturated and glycolated material, and 300 for all other patterns. Clay fractions are clearly dominated by kaolinite (K) and smectite (Sm). I, illite; P, pyrophyllite; Py, pyrite; C, cristobalite; A, alunite; G, gypsum; S, sulfur; Q, quartz; T, tridymite.

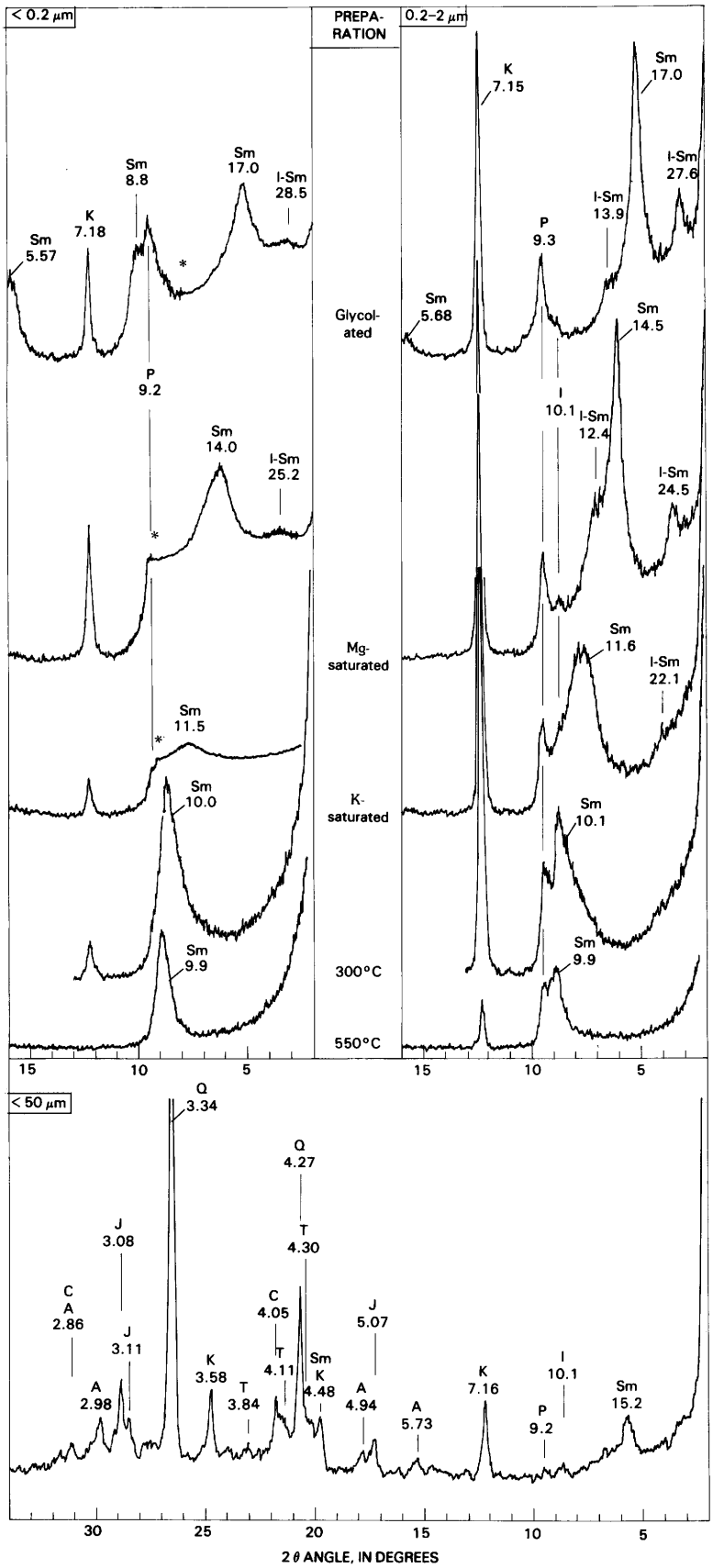

FIGURE 10.—X-ray diffraction patterns of sample Bd-26-1 from tephra Shb1 collected from south rim of Sherman Crater. The <50-μm pattern is from an unoriented mount; clay patterns are from oriented mounts. Scale range is 300 for the pattern of <50-μm material and 1000 for other patterns except for 10,000 on the low-angle side of the asterisks. Clay fractions contain several clay minerals of which kaolinite (K) and smectite (Sm) are the most prominent. I, illite; P, pyrophyllite: I-Sm, mixed-layer illite-smectite; C, cristobalite; A, alunite; J, jarosite; Q, quartz, T, tridymite.

(shb2) prior to deposition is unlikely because of the abundance of physically undisturbed, yet mineralogically altered, lithic lapilli that are pseudomorphic after andesite. The alteration of the upper part of this tephra as indicated particularly by the abundant smectite may have developed during cooling of a once-hot pyroclastic deposit. An alternative cause of intensive alteration could be weathering. Such weathering, however, would not necessarily imply a particularly long period of alteration, as acidic precipitation of both rain and snow is ubiquitous in Sherman Crater owing to emission of sulfurous fumarolic vapor. (Several samples of snowmelt that I have examined in and around Sherman Crater have pH values of less than 4). Acidic solutions from snowmelt or rain could have greatly accelerated weathering processes and altered the fine-grained primary minerals or the glassy matrix to smectite.

On the basis of the next-to-youngest stratigraphic position of shb2 on the crater rim, I infer that this tephra correlates with the second youngest tephra (500–6,000 years B.P.) at the base of the volcano (table 1). The

TABLE 3.—*Minerals identified by X-ray diffraction analysis of two recent tephras from Sherman Crater*

[M, X, T: major, minor, and trace diffraction peaks, respectively]

Size fraction, in micrometers (μm)	Smectite	Mixed-layer illite-smectite	Illite	Pyrophyllite	Kaolinite	Alunite	Jarosite	Quartz	Tridymite	α-Cristobalite	Opal-CT	Feldspar	Gypsum	Sulfur
Sample No. Bd-26-1; deposit shb1, south rim of Sherman Crater														
Lapilli	X				T	M		M			X	T	M	
50–2000	T	T		T	T	T	T	M	X	M		T	X	T
5–50	T	T	T	T	T	X	X	M	X	X		T		T
2–5	M	M		X	M	X		M	T	X		X		
0.2–2	M	M	X	M	M	T		M				T		
<0.2	M	M		M	M									
Sample No. BBB-2; deposit shb1, Landes Cleaver														
50–2000	T		T	T	T	X	T	M	X	X		T		
5–50	T		T	T	X	X		M	X	X		T		T
2–5	M	X	X	X	M	X		M	T	X		X		
0.2–2	M	M	M	M	M			X				T		
<0.2	M	M	M	M	M									
Sample No. Bd-26-2; deposit shb2, south rim of Sherman Crater below Bd-26-1														
Lapilli	M						T				T	M	M	
50–2000	X										X	X		
5–50	X						X				X	T		T
2–5	M				T						T	T		
0.2–2	M				X									
<0.2	M				T									

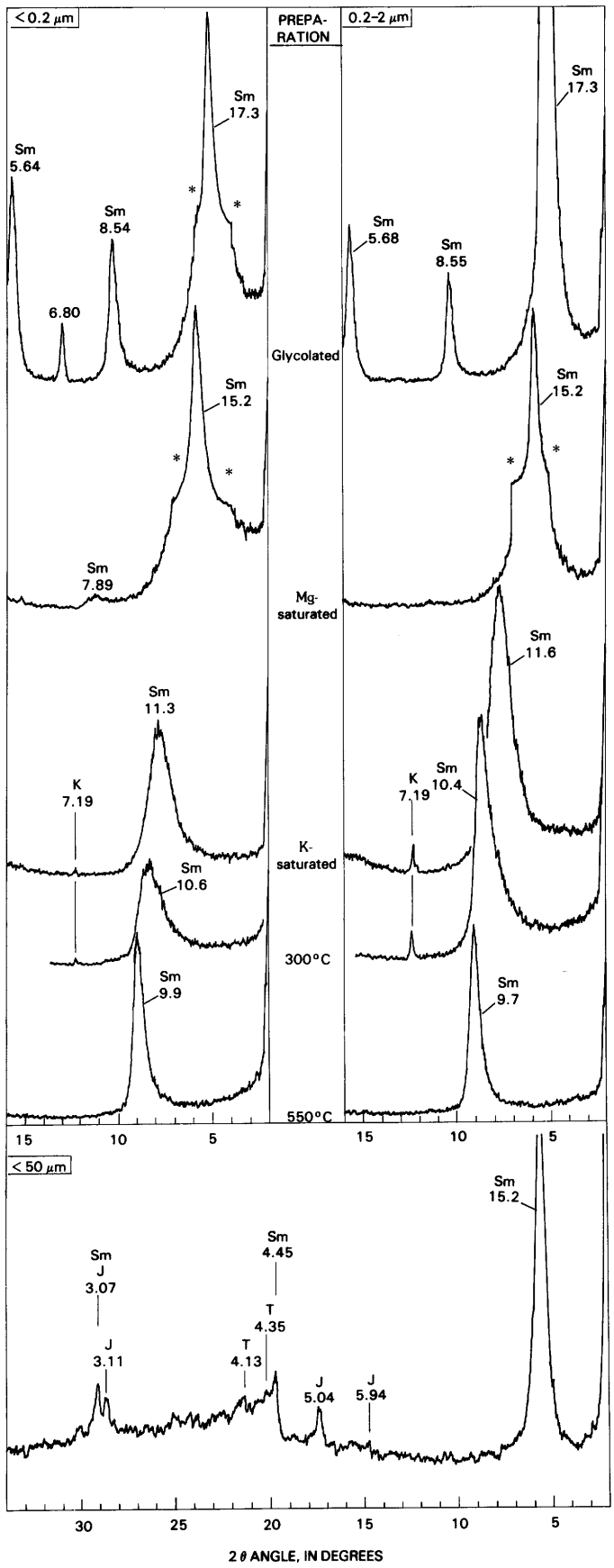

FIGURE 11.—X-ray diffraction patterns of sample Bd-26-2 from breccia shb2 collected from south rim of Sherman Crater. The <50-μm pattern is from an unoriented mount; clay patterns are from oriented mounts. Vertical-scale range is 300 for the pattern of <50-μm material, and 1,000 for other patterns, except for 10,000 between the asterisks. Clay fractions are dominated only by smectite (Sm). K, kaolinite; J, jarosite; T, tridymite.

dominant mineral in the silt and clay fractions of the tephra at the base of the cone is feldspar; no significant quantities of clay minerals were identified. The mineralogy, therefore, is not useful for correlation because of the high degree of post-eruptive alteration at Sherman Crater.

Extensive analyses of clay minerals were not made for older deposits in Sherman Crater. In general, oxidation to a bright yellow, tan, brown, or red is prevalent on the surfaces of rocks exposed in the crater, presumably because of hydrothermal effects. This coloration is in marked contrast to the generally gray, although locally red, lava flows, sills, and breccias that form most of Mount Baker. Thin sections of porphyritic rock from the crater rim, near the east breach, and near the crater lake show feldspar phenocrysts replaced to various degrees, and thin sections also show veins and vesicles commonly filled with fine-grained minerals. Once-glassy or fine-grained groundmasses are usually isotropic and retain little original texture. XRD examination of crushed rocks shows that dominant crystalline components are alunite, gypsum, and in some samples feldspar, with lesser amounts of cristobalite and pyrite. Only a small amount of smectite occurs in some samples, and no significant kaolinite is present.

In summary, alunite and a silica phase—either opal, cristobalite, tridymite, or quartz—are widespread fine-grained alteration products in deposits on the rim of Sherman Crater and in vent-filling debris. Clay minerals are most abundant in the matrix of the rim deposits. Kaolinite, in particular, is found mainly in tephra that represents vent-filling debris that was previously altered at some depth prior to eruption. Although present, kaolinite seems to be much less abundant in material altered in situ at the surface of vent-filling debris than at depth.

DORR FUMAROLE FIELD

The Dorr Fumarole Field contains more than 3000 m^2 of currently active thermal ground located midway up the north side of Mount Baker (fig. 2). Exposed, warm ground extends from the inner part of a small cirque at the head of Mazama Glacier to the north along a gently sloping ridge beside the east margin of the glacier. At the south end of the area, sulfurous vapors issue from numerous joints in a lava flow exposed along the southeast wall of the cirque. Abundant meltwater from snow and ice courses over the cirque wall in rivulets which lead to small ice caves in Mazama Glacier. In transit, meltwater forms many sputtering pools in the debris around fumaroles. A blanket more than 50 cm thick of gravelly to clayey debris extends 150 m along the adjacent ridge. Material on the ridge is baked dry by ground heat to a much greater extent than exposures on the cirque wall, and cavities in the ridge debris commonly contain sulfur rosettes with blades as much as a few centimeters long.

Samples of the clayey debris are mineralogically similar to the white tephra (shb1) from Sherman Crater. Cream-colored material contains abundant quartz and smectite, with lesser kaolinite and alunite. A sample of orange material is similar but with abundant jarosite and less alunite and kaolinite. At least some of the surficial debris may correlate with shb1 in Sherman Crater. However the thickness of debris suggests that additional material may have been erupted from a previously active vent at the site of the Dorr Field.

Abundant blocks of porphyritic andesite are incorporated into the debris, and their surfaces are outwardly bleached to white or pink. Feldspar phenocrysts are much less altered than similar material in Sherman Crater, and fine-grained veins are only sparsely present.

LATE QUATERNARY MUDFLOWS AND AVALANCHES

The mineralogy of the matrix and pebble-size material from mudflow and avalanche deposits at the foot of Mount Baker was examined by XRD analysis (table 4). Samples were collected by J. H. Hyde from deposits (table 1) described by Hyde and Crandell (1978). As a basis for interpretation of the origin of these deposits, the silica-kaolinite-alunite (or jarosite) assemblage is assumed to be the product of hydrothermal alteration involving sulfuric acid solutions. The kaolinite component of this assemblage should not result from weathering in a normal alpine environment. For example, although Reynolds (1971, p. 366–367) found chemical weathering to be a significant process in alpine areas near South Cascade Glacier, 70 km southeast of Mount Baker, he found no unequivocal evidence of kaolinite; the dominant clay minerals in weathering products were vermiculite, mixed-layer vermiculite-phlogopite, and smectite. A study by Bockheim (1972, p. 104–105) of soil-forming processes in the Mount Baker area proper, showed that vermiculite was the dominant weathering product in the clay fraction of soils north of Mount Baker. Only a small amount of kaolinite was found in these soils, and Bockheim (1972, p. 108) believed the kaolinite to be originally from parent material in the shale bedrock at that locality. I concur that the kaolinite is from parent material, although examination of a photograph of one of Bockheim's (1972, p. 27) soil profiles suggests that the kaolinite more likely came from a white tephra (probably unit shb1) near the top of the profile. At any

rate, kaolinite is unlikely to be an abundant authigenic weathering product of Holocene deposits at the base of Mount Baker.

Smectite may also originate from hydrothermal alteration, but it is not as good an indicator of hydrothermal origin as is kaolinite. Smectite has been reported as a weathering product of volcanic glass in a large number of different environments (Millot, 1970, p. 47), and it does not require strongly acidic solutions for formation. Mullineaux (1974, p. 67) considered smectite to be of hydrothermal origin, however, in the 5700-year-old Osceola Mudflow and associated tephra at Mount Rainier because of the typical lack of this clay mineral in other weathered Holocene tephra. More extensive sampling and clay analysis of Holocene tephra and soils at the base of Mount Baker might show that smectite there also is not a prominent weathering product and thus may be indicative of hydrothermal origin.

Table 4 shows that, except for sample SM3, the alteration assemblage of silica-kaolinite-alunite (or jarosite) is prominent in the matrices of only the younger (≤600 years B.P.) mudflows. These include two in Boulder Creek (sample Nos. B3, B4) and one in Park Creek (sample No. P1). Examples of the XRD patterns of fine fractions from these deposits are shown in figure 12*A*. In older mudflows the assemblage, if present, is prominent only in the clasts, and kaolinite is never dominant (fig. 12*B*). XRD analysis of the clay fractions of most of these older mudflows reveals only trace components of clay minerals including smectite, illite, chlorite, and, in one sample, pyrophyllite.

An exception is a deposit in the Baker Pass area (sample No. SM3) believed by Hyde and Crandell (1978, p. 10) to be a thin veneer that correlates with the large Middle Fork Nooksack River mudflow (sample No. M2). Sample SM3 contains a significant though not dominant component of kaolinite and alunite in the matrix. Most of this mudflow traveled down the Middle Fork Nooksack River and Sulphur Creek (Hyde and Crandell, 1978, p. 10), and samples from these localities (samples M2 and SM2, respectively) probably better represent the bulk of the mudflow. Sample SM3 must represent a relatively small but much more altered mass incorporated into the bulk of the mudflow.

The young Rainbow Creek avalanche (sample No. R1) is distinctive because it contains abundant smectite in both the matrix and clasts. The smectite is not considered to result expressly from alteration in or near a volcanic vent, because of the likelihood that the avalanche originated in cliffs within the Rainbow Creek valley well away from known vent areas.

Figure 13 shows the temporal distribution of hydrothermally altered material in the large mudflows and avalanches from Mount Baker. Younger mudflows originated from kaolinite-rich parts of the upper cone; older mudflows did not.

Conclusions on dependent variations between altered material and the magnitude or frequency of large mass movements are more speculative. Table 1 and figure 13 show that the magnitude of mudflows decreased somewhat with increase in the amount of clay, although the younger mudflows are nevertheless

TABLE 4.—*Minerals identified by X-ray diffraction analysis of large Holocene mudflows and avalanches from Mount Baker*

[M, X, T: major, minor, and trace diffraction peaks, respectively. Samples were collected by J. H. Hyde]

Deposit and size fraction, in micrometers	Smectite	Illite	Chlorite	Pyrophyllite	Kaolinite	Alunite	Jarosite	Quartz	Tridymite	α-Cristobalite	Opal-CT	Feldspar	Gypsum	Pyrite	Zeolite	Amphibole	Pyroxene	Olivine
Sample No. B3; mudflow in Boulder Creek valley; a few hundred years old																		
Clasts[1]					M			M				X						
50–2000 μm								M				M						
4–50 μm					T	T		M				X						
<4 μm	X	T	T	T	X	X	T	M				X						
Sample No. R1; avalanche in Rainbow Creek valley; a few hundred years old																		
50–2000 μm	X											M						
4–50 μm	X											M						
<4 μm	M											X						
Sample No. B4; mudflow in Boulder Creek valley; a few hundred years old																		
Clasts					M	X		M	X		X				T			
50–2000 μm						T		M				M				T		
4–50 μm					T	T		M	X	M		X						
<4 μm					X	X	T	M	T	X		T						
Sample No. P1; mudflow in Park Creek valley; 500–600 years old																		
Clasts	T	X		T	M			M				T			T			
50–2000 μm			T					M			T	M						
4–50 μm			T				T	M			X	T						
<4 μm	M		T	X	M		X	X			T							
Sample No. M1; mudflow in Middle Fork Nooksack River valley; 300–6000 years old																		
Clasts								X			M							
50–2000 μm								X				M					X	
4–50 μm								M				M						
<4 μm	T										T	X						
Sample No. M2; mudflow in Middle Fork Nooksack River valley; 6000 years old																		
Clasts	T	T	T	T	X	M			M	M			T	T		X	M	M
50–2000 μm		T	T					M				M						
4–50 μm		T	T					M	T	X		X						
<4 μm	T	T	T	T				X				X						
Sample No. SM2; mudflow in Sulphur Creek valley; 6000(?) years old																		
Clasts					X					X								
50–2000 μm			T									M	T			T		
4–50 μm										T		M	T					
<4 μm										T		M						
Sample No. SM3; mudflow at Baker Pass; 6000(?) years old																		
Clasts				X	X	M		M	M	X	X	M						
50–2000 μm						X		X	X	M		M						
4–50 μm	T					X		X	X	X			T					
<4 μm	X				X	X		T	T	X								
Sample No. P2; mudflow in Park Creek valley; 6200–6600 years old																		
Clasts					X	X			X	X								
50–2000 μm			T					X				M				T		
4–50 μm			T					X				X						
<4 μm			T					X				X						
Sample No. SM1; mudflow in Sulphur Creek valley; 6600–10,400 years old																		
50–2000 μm												M						
4–50 μm												M						
<4 μm												X						

[1]Light-colored, fine-grained clasts of pebble size were selected from the bulk samples for separate analysis. This row includes the combined analyses for several clasts.

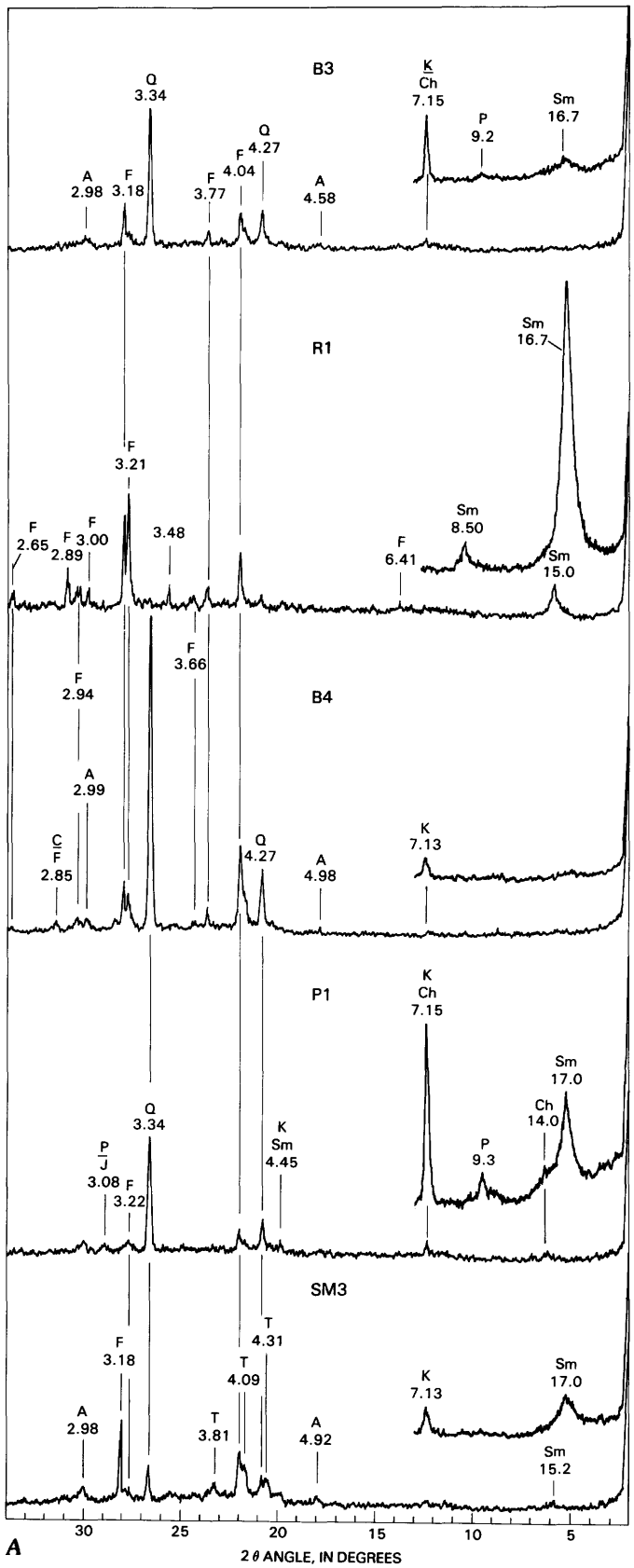

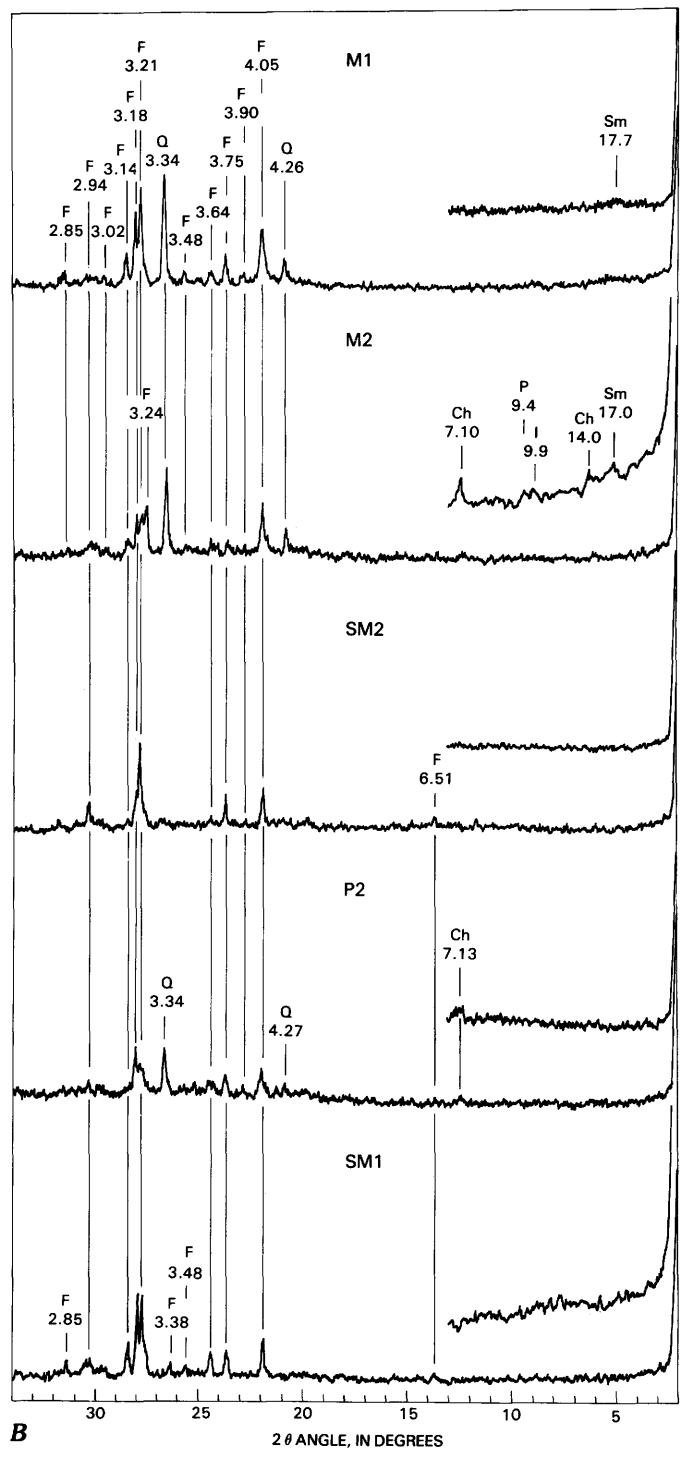

FIGURE 12.—X-ray diffraction patterns of Holocene mudflows at Mount Baker. Long patterns are of unoriented 4–50-μm splits; short patterns are of oriented and glycolated <4-μm splits. Clay minerals were identified by heat treatments (not shown) and glycolation. Where peaks for two minerals overlap, the dominant mineral is underlined. Vertical scale range is 1,000 for all patterns, except for samples M2 and SM1 for which range is 300 for the <4-μm pattern.

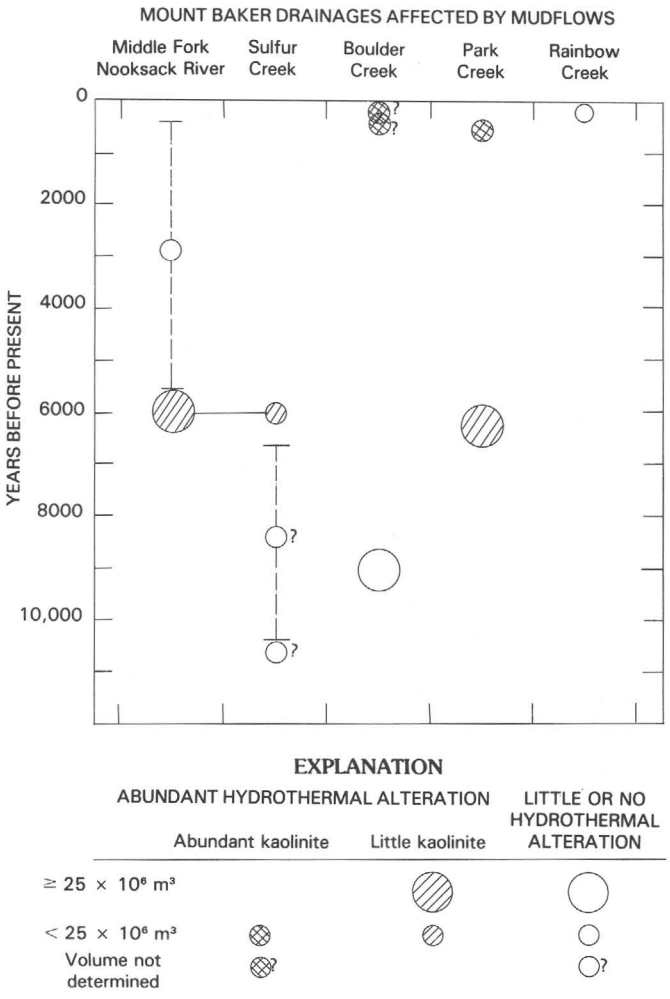

FIGURE 13.—Distribution of hydrothermal products in valley deposits of large mudflows and avalanches from Mount Baker. Samples of the oldest mudflows in Boulder and Sulphur Creek valleys were not examined for this report; however, Hyde and Crandell (1978, p. 6, 9) noted an absence of alteration products in the older mudflows of the Boulder Creek assemblage and less than 10 percent altered rock fragments in the oldest Sulphur Creek mudflow.

EXPLANATION FOR FIGURE 12

A, Younger mudflow and avalanche deposits. These samples contain large amounts of clay minerals in the clay fraction. In particular, kaolinite (K) is present in the clay fraction of the three youngest mudflows from Sherman Crater—represented by samples B3, B4, and P1. Kaolinite is also present in sample SM3, believed to be from a relatively minor deposit that correlates with the sources of samples M2 and SM2.

B, Older Holocene mudflows. Sample SM1 has a short XRD pattern of an untreated <4-μm split. These older samples do not contain significant amounts of clay minerals in the clay fractions. A, alunite; F, feldspar; Q, quartz, Ch, chlorite; P, pyrophyllite; Sm, smectite; C, cristobalite; J, jarosite, T, tridymite; I, illite.

of catastrophic proportions. With respect to the frequency of mudflows, most are not evenly spaced through time but instead seem to be clustered during four time periods (table 1): at least one mudflow more than 10,000 years ago; more than 16—mostly associated with pyroclastic flows—about 9,000 years ago; at least two between 6,000 and 7,000 years ago; and at least three mudflows and one avalanche during the last 600 years. The remaining two mudflows are poorly dated and could fall during or between these periods. Occurrences of those events that are reasonably well dated and are not known to be accompanied by eruptive deposits increased from two between 6,000 and 7,000 years ago to four in the last 600 years. Considering only those mudflows that contain hydrothermally altered material, occurrences increased from two between 6,000 and 7,000 years ago, to three in the last 600 years. This record is too sparse to determine the effects of hydrothermal alteration on the frequency of mudflows, especially when other possibly important factors are neglected such as air temperature and precipitation extremes, earthquakes, steam explosions, or eruptions that left no recognizable deposits. However, the data at least suggest a parallel development of increasingly altered source rock and increasing mudflow occurrence. Such a pattern could result when hydrothermal alteration produces rock instabilities relieved by large mass movements.

PROCESS OF ALTERATION

ALTERATION IN CRATER LAKE

A study of solutions leading to hydrothermal alteration in Sherman Crater was aided by the opportune formation of an accessible crater lake that accompanied the 1975 increase in thermal activity. The lake formed during April from melted snow and ice in a shallow basin at the bottom of a 30–40-m deep ice pit near the center of Sherman Crater (fig. 14). The maximum depth of the lake was estimated by probing to be about 2 m in August 1976 (E. P. Kiver, written commun., 1978). The area of the lake gradually decreased after 1975. The area of the central ice pit also decreased as a result of a localized decrease in thermal activity. Frank, Meier, and Swanson (1977) estimated an initial volume of 2600 m³ in September 1975. By October 1976, the estimated volume decreased to about 1000 m³. The lake basin was temporarily covered by an ice avalanche from the north rim of the crater in 1977 and was completely covered by seasonal snow by 1979. A buried pond possibly remains beneath the firn in a manner

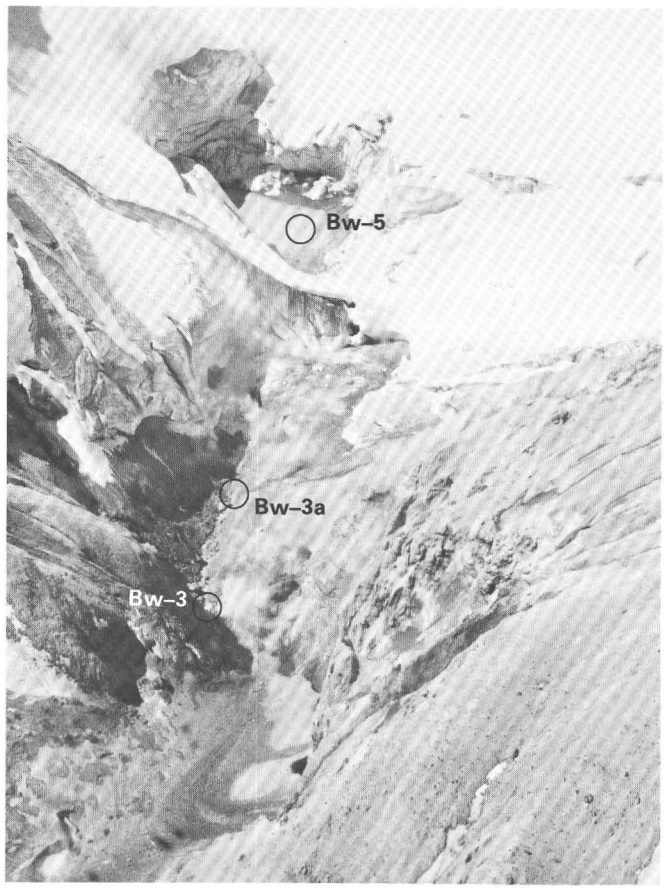

FIGURE 14.—Lake and creek in Sherman Crater as viewed through the east breach toward the west on August 30, 1976. Outlet stream flows toward the camera through the east breach and into the head of Boulder Glacier. Open circles designate sampling sites; Bw-5 in lake, Bw-3 (lowermost) and Bw-3a in creek. Lake and upper creek sites are about 130 m apart.

similar to the subglacial lake thought to have existed for many years prior to 1975 (Frank and others, 1975, p. 86).

The major water inflow to the lake basin consists of snow- and ice-meltwater from other areas of the crater, mainly from fumarole clusters west and northwest of the lake. The only observed outflow travels eastward through an ice tunnel and then reappears as it skirts a highly active fumarole cluster near the east breach of the crater rim (fig. 14). Prior to reaching the east breach, the outflow creek mixes with additional water from other parts of the crater and then in a single stream plunges beneath ice in the east breach. The stream travels subglacially down the east slope of Mount Baker and forms part of the headwaters of Boulder Creek at the terminus of Boulder Glacier.

The chemistry of the crater lake is affected by a number of factors. The most important are probably reactions with the lake sediment and with effluents from one or more submerged fumaroles, the largest of which appears as an area of strong upwelling about 2 m across near the center of the lake. Other factors include (1) effluents from fumaroles on or near the lakeshore, (2) the few streams from other areas of the crater, (3) acidic precipitation of rain and snow owing to the oxidation and hydrolysis of sulfurous gases present in the crater environment, and (4) air-fall accumulation of fumarole ejecta, which in the summer of 1975 amounted to a layer about 1 cm thick near the lake. The lake temperature is affected by most of these factors as well as by evaporation, air temperature, and conductive heat transfer from the lake floor (Friedman and Frank, 1980, p. 24–26).

Water samples were collected from the crater lake on June 11 and August 8, 1975, by casting a container into the lake from the top of the ice pit. Samples also were collected on different dates in 1974 and 1976 from the crater creek 130–140 m downstream from the lake, and from Boulder Creek about 5 km downstream from the lake. Temperature and pH measurements were made in the field. Major ions were determined at U.S. Geological Survey laboratories in Tacoma and Salt Lake City, and are listed by Bortleson, Wilson, and Foxworthy (1977, table 1) and by G. C. Bortleson (written commun., 1976). Temperatures of the two lake samples, 26° and 34°C, respectively, are comparable to temperatures measured at other times during September 1975 and August 1976 (S. D. Malone, oral commun., 1976) and roughly represent the equilibrium temperature between geothermal emission, meltwater inflow, calving ice, and the atmosphere.

Tables 5, 6, and 7 list chemical data for the water samples. Activities (a) are the products of the molalities (m) and the activity coefficients (γ) that were derived from the Debye-Huckel equation by methods outlined by Garrels and Christ (1965, p. 61–62). The ionic strength (I) of each sample is calculated by assuming that

(1) at the low pH values, sulfur species existed in solution as a mix of SO_4^{-2} and HSO_4^{-1} which are determined by solving two equations,

$$\frac{a_{H^{+1}}\, a_{SO_4^{-2}}}{a_{HSO_4^{-1}}} = 10^{-1.9} \text{ and } m_{SO_4^{-2}} + m_{HSO_4^{-1}} = \Sigma m_{SO_4^{-2}}$$

where $\Sigma m_{SO_4^{-2}}$ and $a_{H^{+1}}$ are given by the water analyses;

TABLE 5.—*Chemistry of the crater lake at Sherman Crater*

[Analytical data are from Bortleson, Wilson, and Foxworthy (1977, table 1). Values with a superscript, T, are total recoverable species, dissolved and suspended; all other values are dissolved species. Parentheses indicate concentration values which are calculated by methods described in the text. mg/L, milligrams per liter; *m*, molality; *a*, activity; γ, activity coefficient; leaders (...), not determined or analytical value not used; μho, micromho]

Sample No.	Bw-5-1				Bw-5-2			
Date	June 11, 1975				Aug. 8, 1975			
Time (local)	1000				0900			
Constituent	mg/L	$m\times10^3$	γ	log *a*	mg/L	$m\times10^3$	γ	log *a*
H^{+1}	(3.7)	(3.7)	0.85	−2.5	(4.6)	(4.6)	0.87	−2.4
K^{+1}	24	.61	.80	−3.31	13	.33	.83	−3.56
Na^{+1}	88	2.8	.81	−2.51	73	3.2	.84	−2.57
Ca^{+2}	130	3.2	.47	−2.82	98	2.4	.52	−2.90
Mg^{+2}	37	1.5	.51	−3.12	22	.91	.55	−3.30
Mn^{+2}	...	...	...	...	.96[T]	.017	.52	−5.05
Fe^{+2}	(38)	(.68)	.47	−3.50	19[T]	.34	.52	−3.75
Al^{+3}	(76)	(2.8)	.23	−3.19	38[T]	1.4	.28	−3.41
ΣSO_4^{-2}	1300	14	...	...	960	10	...	...
SO_4^{-2}	(1200)	(12)	.44	−2.28	(810)	(8.4)	.49	−2.39
HSO_4^{-1}	(170)	(1.7)	.81	−2.86	(160)	(1.6)	.84	−2.87
Cl^{-1}	28	.79	.80	−3.20	28	.79	.83	−3.18
F^{-1}	4.8	.25	.81	−3.69	27	.14	.83	−3.93
B	.20[T]	.019	...	...	2.5[T]	.23	...	...
SiO_2	220	3.7	1.0	−2.43	140	2.3	1.0	−2.64

Sample No.	Bw-5-1	Bw-5-2
Date	June 11, 1975	Aug. 8, 1975
Time (local)	1000	0900
Ionic strength	0.053	0.036
Ionic balance (percent)	+1.0	+0.8
Temperature (°Celsius)	34	26
pH	2.5	2.4
Specific conductance (μmho)	3840	2400

TABLE 6.—*Chemistry of the crater creek at points 140 m (Bw-3) and 130 m (Bw-3a) downstream from the crater lake*

[Analytical data are from Bortleson, Wilson, and Foxworthy (1977, table 1) for 1974, and from G. C. Bortelson (written commun., 1976) for 1976. Values with a superscript, T, are total recoverable species, dissolved and suspended; all other values are dissolved species. Parentheses indicate concentration values which are calculated by methods described in the text. mg/L, milligrams per liter; *m*, molality; *a*, activity; γ, activity coefficient; leaders (...), not determined or analytical value not used; μho, micromho]

Sample No.	Bw-3-1				Bw-3-2				Bw-3a-5			
Date	May 28, 1974				Aug. 17, 1974				July 14, 1976			
Time (local)	1800				0900				1300			
Constituent	mg/L	$m\times10^3$	γ	log *a*	mg/L	$m\times10^3$	γ	log *a*	mg/L	$m\times10^3$	γ	log *a*
H^{+1}	(1.8)	(1.8)	0.89	−2.8	(0.72)	(0.71)	0.89	−3.2	(1.8)	(1.8)	0.87	−2.8
K^{+1}	3.0	.077	.87	−4.17	3.3	.084	.86	−4.14	6.0	.15	.84	−3.90
Na^{+1}	15	.65	.87	−3.25	16	.70	.87	−3.22	44	1.9	.85	−2.79
Ca^{+2}	99	2.5	.60	−2.82	120	3.0	.59	−2.75	141	3.5	.54	−2.72
Mg^{+2}	10	.41	.62	−3.59	12	.49	.61	−3.52	21	.86	.57	−3.31
Mn^{+2}	...	...	...	...	.45	.008	.59	−5.33	.79[T]	.014	.54	−5.12
Fe^{+2}	12	.21	.60	−3.90	18	.32	.59	−3.72	(18)	(.32)	.54	−3.76
Al^{+3}	(27)	(1.0)	.35	−3.46	(26)	(.98)	.34	−3.48	43[T]	1.6	.29	−3.33
ΣSO_4^{-2}	450	4.7	...	...	510	5.3	...	...	660	6.9	...	...
SO_4^{-2}	(410)	(4.3)	.58	−2.60	(490)	(5.1)	.57	−2.54	(610)	(6.4)	.51	−2.49
HSO_4^{-1}	(39)	(.4)	.87	−3.46	(19)	(.2)	.87	−3.76	(49)	(.5)	.81	−3.37
Cl^{-1}	1.6	0.045	.87	−4.41	.9	.025	.86	−4.67	8.8	.25	.84	−3.68
F^{-1}	1.0	.053	.87	−4.34	1.3	.068	.86	−4.23	1.1	.058	.84	−4.31
B	.22	.020	...	...	.12	.011	...	...	.73[T]	.068	...	...
SiO_2	70	1.2	1.0	−2.92	66	1.1	1.0	−2.96	130	2.2	1.0	−2.66

Sample No.	Bw-3-1	Bw-3-2	Bw-3a-5
Date	May 28, 1974	Aug. 17, 1974	July 14, 1976
Time (local)	1800	0900	1300
Ionic strength	0.021	0.023	0.032
Ionic balance (percent)	+13	+7.0	+14
Temperature (°Celsius)	7	8	22
pH	2.8	3.2	2.8
Specific conductance (μmho)	1400	1360	1880

TABLE 7.—*Chemistry of Boulder Creek near the Boulder Glacier terminus at points about 5 km downstream from the crater lake*

[Analytical data are from Bortleson, Wilson, and Foxworthy (1977, table 1) for 1974, and from G. C. Bortelson (written commun., 1976) for 1976. Values with a superscript, T, are total recoverable species, dissolved and suspended; all other values are dissolved species. Parentheses indicate concentration values which are calculated by methods described in the text. mg/L, milligrams per liter; *m*, molality; *a*, activity; γ, activity coefficient; leaders (...), not determined or analytical value not used; μmho, micromho]

Sample No. / Date / Time (local)	Bw-2a-1 May 28, 1974 1830				Bw-2a-2 June 26, 1976 1030			
Constituent	mg/L	$m\times10^3$	γ	log *a*	mg/L	$m\times10^3$	γ	log *a*
H^{+1}	(0.34)	(0.34)	0.94	−3.5	(0.27)	(0.27)	0.92	−3.6
K^{+1}	1.4	.036	.93	−4.48	2.2	.056	.91	−4.29
Na^{+1}	4.7	.20	.93	−3.73	9.1	.40	.91	−3.44
Ca^{+2}	23	.57	.76	−3.36	35	.87	.70	−3.22
Mg^{+2}	5.4	.22	.76	−3.78	7.4	.30	.71	−3.67
Mn^{+2}	...	...	...	...	$.26^T$	.005	.70	−5.46
Fe^{+2}	3.2	.057	.76	−4.36	10^T	.18	.70	−3.90
Al^{+3}	3.0	.11	.55	−4.22	8.7^T	.32	.47	−3.82
ΣSO_4^{-2}	100	1.0	...	...	240	2.5	...	...
SO_4^{-2}	(100)	(1.0)	.75	−3.12	(240)	(2.5)	.69	−2.76
HSO_4^{-1}	(0)	(0)	.93	0	(0)	(0)	.91	0
Cl^{-1}	.9	.025	.93	−4.63	.1	.003	.91	−5.56
F^{-1}	.5	.026	.93	−4.62	.7	.037	.91	−4.47
B	.03	.003	...	...	$.12^T$	.011	...	...
SiO_2	24	.40	1.0	−3.40	80	1.3	1.0	−2.89

Sample No. / Date / Time (local)	Bw-2a-1 May 28, 1974 1830	Bw-2a-2 June 26, 1976 1030
Ionic strength	0.005	0.009
Ionic balance (percent)	+12	−6.8
Temperature (°Celsius)	2	1.7
pH	3.5	3.6
Specific conductance (μmho)	380	570

(2) aluminum species existed at low pH as Al^{+3};

(3) iron existed in the reduced form, Fe^{+2};

(4) $m_{H^{+1}}=\frac{a_{H^{+1}}}{\gamma_{H^{+1}}}$ and $a_{H^{+1}} = 10^{-pH}$; and

(5) ions for which no analyses were made were not major constituents of the solutions.

The ionic balances ($\frac{meq_{cations}-meq_{anions}}{meq_{cations}+meq_{anions}} \times 100$), which should approach zero, suggest that these assumptions are valid for the lake samples (table 5). The imbalance of other samples (tables 6–7) might be explained by the unaccounted presence of complexes. For example, aluminum would be expected to combine to some degree with fluoride and sulfate (Hem, 1968). Particularly calcium, the most abundant cation in the unbalanced samples, might combine with sulfate as an ion pair.

When the lake was sampled on August 8, 1975, part of the water (Bw-5-2) was filtered through a 0.45-μm cellulose filter. Microscopic and XRD analysis indicate that much of the trapped sediment is opal-A. XRD analysis shows that the crystalline components are primarily alunite with lesser amounts of sulfur, quartz, opal-CT, kaolinite, and smectite. A sample of suspended sediment taken from the creek at a point about 130 m downstream from the lake on July 14, 1976 (from Bw-3a-5), is also considered to be representative of lake sediment with additional minerals derived from the creek bed or other nearby streams. The X-ray pattern of the creek sediment is similar to that of the lake sediment but also includes minor peaks of pyrite.

SIGNIFICANCE OF SOLUTION CHEMISTRY OF ALUNITE

Alunite was examined in some detail because it is the major crystalline component of the suspended sediment in the crater lake, and it appears to be a common indicator of intense hydrothermal alteration in Sherman Crater. Two previous studies that relied on XRD

analysis, however, did not identify the presence of alunite in surficial material from Sherman Crater (Bockheim and Ballard, 1975; Eichelberger and others, 1976). The discrepancy is difficult to explain, but it may result from sample collection in different areas by different investigators. The occurrence of alunite in samples that I collected was confirmed by comparison of the X-ray diffraction data with that of numerous other published studies of alunite (for example, Parker, 1962; Slansky, 1973, 1975). Figure 15 shows X-ray patterns of four alunitic samples, including sediment from the crater lake and crater creek, surficial debris from the west rim, and a clast from the 6,000-year-old mudflow (M2) in the Middle Fork Nooksack River valley.

Alunite is an alkalic aluminum hydroxy sulfate, $K_xNa_{1-x}Al_3(SO_4)_2(OH)_6$, in which potassium and sodium exchange to form a solid-solution series between alunite and natroalunite, the respective potassium and sodium end-members (Hendricks, 1937). Jarosite, $KFe_3(SO_4)_2(OH)_6$, is a related mineral in which iron takes the place of aluminum in the alunite structure (Hendricks, 1937; Brophy and others, 1962). Although common in some deposits at Mount Baker, jarosite is not nearly as widespread as is alunite.

The mole fraction of potassium (x) in alunite can be determined from the work of Parker (1962, p. 134) who measured a displacement of the [006] diffraction peak of the unit-cell *c*-dimension with a variation of mole fraction. For the Mount Baker samples, x is variable. Alunite in the lake and creek sediment (fig. 11) has an [006] peak at 2.85Å that corresponds to $K_{0.6}Na_{0.4}$-alunite according to Parker's (1962, p. 134) graph. Surficial debris from the west rim and the mudflow clast have an [006] peak at 2.88Å for $K_{0.9}Na_{0.1}$-alunite. For the stability calculations described later, potassium mole fractions of 0.6 and 1 are used for alunite in crater solutions.

Alunite is not unusual in contact with acid-sulfate water, and some studies suggest that alunite can precipitate directly from natural solutions. Zotov (1967) found 35–40 percent alunite in 6–8 m of mud at the bottom of Kipyashcheye Lake on Golovnin volcano. He believed that alunite formed by the precipitation reaction:

$$0.6K^{+1}+0.4Na^{+1}+3Al^{+3}+2SO_4^{-2}+6H_2O \rightleftarrows K_{0.6}Na_{0.4}Al_3(SO_4)_2(OH)_6+6H^{+1}.$$

Zotov (1967, p. 125) identified the mineral as

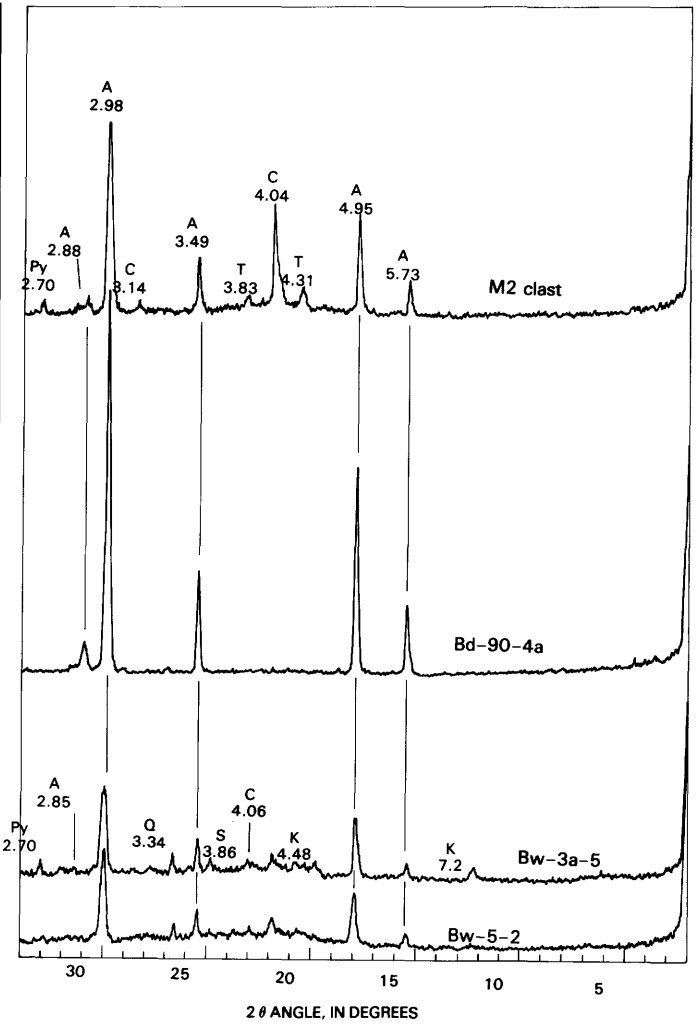

FIGURE 15.—X-ray diffraction pattern of selected samples that contain alunite (A). Samples include suspended sediment filtered through cellulose filters (0.45-μm openings) from the crater lake (Bw-5-2) and the crater creek (Bw-3a-5), surficial debris collected within an alteration zone 5 m away from a major cluster of fumaroles on the west rim (Bd-90-4a), and a hydrothermally altered clast (≈1 cm across) from the 6,000-year-old mudflow (sample No. M2) in the Middle Fork Nooksack River valley. The suspended sediment and the clast were lightly ground, and the surficial debris was split at 50 μm prior to X-ray analysis in unoriented mounts. Vertical-scale range is 1000 for all patterns. The sample from the west rim is almost pure alunite except for a few trace peaks at low angles. Major crystalline component in the other samples is also alunite, although several other minerals are present. The suspended sediment contains, in addition to crystalline components, a large amount of amorphous material, much of which is opal-A as indicated by microscopic examination and by the low broad hump centered at the 4Å-cristobalite (C) peak in the XRD pattern. Py, pyrite; Q, quartz; S, sulfur; T, tridymite; K, kaolinite.

$K_{0.6}Na_{0.4}$-alunite. This analysis is the closest analogue that I have found in the literature to conditions at Mount Baker. The primary difference is of scale. The Russian lake is larger, and the concentrated mud deposit is probably much thicker than at Mount Baker. Also the Kipyashcheye Lake water has much greater concentrations of Na^{+1} and Cl^{-1}, although the $\frac{K^{+1}}{Na^{+1}}$ ratio in solution as well as in alunite is similar to that at Mount Baker's crater lake (<0.2 in solution and about 1.5 in alunite at both localities).

In the Paint Pot Hill area of Yellowstone National Park, Raymahashay (1968) examined rock alteration in mudpots, pools, and springs and found alunite to be a major product. He represented alunite formation by the same precipitation reaction as Zotov (1967), as well as by alteration of kaolinite (Raymahashay, 1968, p. 508):

$$3Al_2Si_2O_5(OH)_4+2K^{+1}+6H^{+1}+4SO_4^{-2}+9H_2O \leftrightarrows 2KAl_3(SO_4)_2(OH)_6+6H_4SiO_4.$$

Raymahashay (1968, p. 521) concluded from field observations and solution chemistry that nearly pure K-alunite was precipitating in the acid springs and that in these waters kaolinite should readily alter to alunite.

In New Zealand, Slansky (1975) found mixtures of potassium- and sodium-rich alunite minerals on the crater floor and on the walls of boiling pools at White Island volcano. He tentatively concluded (p. 291) from the lack of observed bedding that the minerals were formed by alunitization of preexisting rocks rather than by precipitation from solutions. However, studies by Narebski and Paulo (1973, p. 74–76) of alunitized andesite at Cotopaxi volcano, Ecuador, suggest that even in these types of altered rocks, alunite is a precipitation product as it exists mainly in veins and vesicles and only subordinately as feldspar pseudomorphs. Regardless of the type of formation, the necessary requirement in all these examples is a strong sulfate and moderate alkali-ion activity.

The equilibrium relationship of alunite in lake water can be examined (Raymahashay, 1968) by calculating the reaction quotient ($Q_{alunite}$) from the water chemistry and comparing it to the solubility constant of alunite ($K_{alunite}$) predicted by free-energy considerations. This comparison can determine whether the alunite solubility reaction is a control on the water chemistry, and whether the tendency in this reaction is for alunite to precipitate or to dissolve in the lake water. Thermodynamic data used for these and further calculations below are listed in table 8.

Figure 16 shows the solubility of alunite using two solubility constants, one based on the free energy of pure K-alunite and one based on estimates by Zotov (1967, p. 126) of the free energy of $K_{0.6}Na_{0.4}$-alunite. In figure 16, values of Q for the Mount Baker crater lake are similar to those of Kipyashcheye Lake and plot within the precipitation field of $K_{0.6}Na_{0.4}$-alunite. The Q values suggest stability of $K_{0.6}Na_{0.4}$-alunite in both the crater lake and creek at Mount Baker. Values of Q for Yellowstone waters (Raymahashay, 1968, p. 513) tend more toward the precipitation field for K-alunite, which is well in accord with Raymahashay's observation that K-alunite formed a thin layer of precipitate

TABLE 8.—*Free energies of formation and entropies of species in their standard states, for stability calculations of alunite and kaolinite*

Substance	Formula	$S°_{298K}$ $\left(\frac{J}{mol \cdot K}\right)$	$\Delta G°_{f,298K}$ $\left(\frac{J}{mol}\right)$	Reference[1]	
				$S°_T$	$\Delta G°_{f,T}$
K-alunite	$KAl_3(SO_4)_2(OH)_6$	328.03	[2]−4669900	b	a
$K_{0.6}Na_{0.4}$-alunite	$K_{0.6}Na_{0.4}Al_3(SO_4)_2OH)_6$		[2]−4681800		c
Kaolinite	$Al_2Si_2O_5(OH)_4$	203.05	−3799364	b	b
Na-montmorillonite	$Na_{0.33}Al_{2.33}Si_{3.67}O_{10}(OH)_2$		[2]−5368700		a
Muscovite	$KAl_3Si_3O_{10}(OH)_2$		−5600671		b
Microcline	$KAlSi_3O_8$		−3742330		b
Dissolved silica	H_4SiO_4	180.00	−1308000	b	b
Potassium ion	K^{+1}	101.04	−282490	b	b
Sodium ion	Na^{+1}	58.41	−261900	b	b
Aluminum ion	Al^{+3}	−308.00	−489400	b	b
Sulfate ion	SO_4^{-2}	20.00	−744630	b	b
Water	H_2O	69.95	−237141	b	b

[1]a, Raymahashay (1968); b, Robie, Hemingway, and Fisher (1978); c, Zotov (1967).

[2]$\Delta G_f°$ calculated from $\Delta G_r°$ values in the respective references.

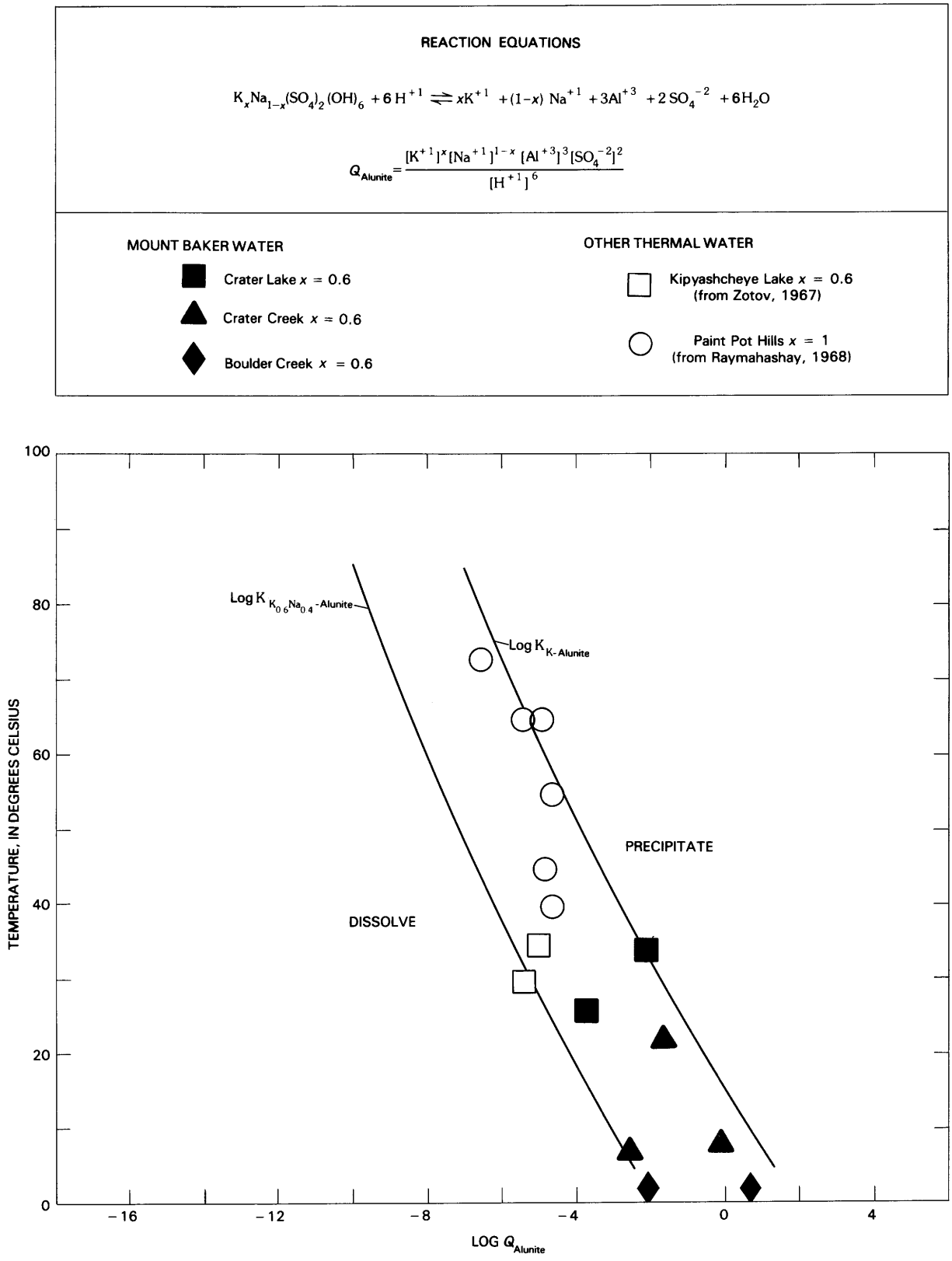

FIGURE 16.—Alunite solubility in acid-sulfate waters. Entropy change ($\Delta S^\circ_{r,T}$) for the solubility reaction is assumed to be constant and to be the same for both K-alunite and $K_{0.6}Na_{0.4}$-alunite. Free energy at other than 25°C (298K) is approximated by $\Delta G^\circ_{r,T} = \Delta G^\circ_{r,298K} - \Delta S^\circ_{r,298K}(T-298K)$.

that covered sinter in one of the springs. Figure 16 indicates that with continuing sulfate production, alunite should precipitate from the crater lake at Mount Baker.

Similar calculations show that $K_{0.6}Na_{0.4}$-alunite is stable relative to kaolinite (fig. 17), Na-montmorillonite, muscovite, and feldspar under the ion-activity conditions of the crater lake. From the solution chemistry, I conclude that the crater lake as well as surficial solutions in other areas of Sherman Crater probably are capable of either producing alunite or maintaining it once it has formed by other means such as direct rock alteration. Futhermore, other alteration products, particularly kaolinite, should be unstable in surficial solutions in Sherman Crater.

MODEL OF NEAR-SURFACE ALTERATION ZONE

The conclusions from solution chemistry are supported by the distribution of hydrothermally altered material. At Mount Baker, kaolinite is most abundant in tephra and fumarole ejecta that represent material formed at some depth beneath surface. Kaolinite is less abundant in the remaining surficial debris and altered rock on the crater rim. These relations suggest that a surficial silica-alunite zone of alteration is underlain by a silica-kaolinite-alunite zone of alteration.

The distribution of altered material in Sherman Crater is somewhat analogous to the Steamboat Springs, Nev., geothermal area, where a highly leached surficial zone of alteration is dominated by acid-sulfate waters derived from oxidation of H_2S gas (Schoen and others, 1974). Similar zones have been described in many other geothermal areas (for example, Steiner, 1953, 1968; Yamasaki and others, 1970).

Figure 18 shows a simple model of a surficial alteration zone as envisioned by Schoen, White, and Hemley (1974, p. 16). A cap of siliceous residue extends down to a water table that marks a transition into a zone rich in alunite and kaolinite. At greater depths with higher pH and less leaching, a smectite zone can become dominant. A similar scheme with some modifications can be applied to Mount Baker (fig. 19). Here, abundant snow and ice provide much meltwater at the surface. The surficial meltwater is acidified by oxidation of H_2S gas in condensed steam around the fumaroles. Poor drainage and meltwater dilution, however, inhibit complete leaching to a solely siliceous residue, and alunite accompanies silica at a surface. Other alteration products are also present but to a lesser degree. Extensive leaching to silica alone might occur locally around fumarole conduits where much of the water is boiled off. For example, siliceous envelopes occur at Cotopaxi volcano, Ecuador, where Narebski and Paulo (1973, p. 72) reported fumarole vents near the surface to be thinly sheathed by sulfur surrounded by a thicker opal envelope that extended outward into an alunite zone.

The lateral extension of the surficial alteration zone at Mount Baker is masked by the altered tephras (shb1 and shb2) which blanket the crater rim. Outside the crater, alteration is likely limited by the absence of fumarole emission; whereas, within the concentric fumarole zone (pl. 1), hydrothermal alteration is probably pervasive. The potential depth of underlying kaolinite- and smectite-rich parts of the alteration zone is unknown, but studies of other geothermal areas that have been penetrated by drill holes indicate what depths are possible. If Schoen, White, and Hemley (1974, p. 16) are correct in their interpretation that the alteration sequence at Ugusu, Japan (Iwao, 1968), is a result of descending sulfuric acid, then such clay-rich products of near-surface alteration can extend as deep as 700 m. Sumi (1970, p. 506) reported that zoned kaolinite and montmorillonite occur at least 900 m deep at the Matsukawa geothermal area. Yamasaki, Matsumoto, and Hayashi (1970, p. 206) found major amounts of these minerals at least 700 m deep at the Otaki geothermal area.

Hydrothermally derived clay deposits at Sherman Crater could presumably extend to depths at which temperatures become too great for kaolinite and montmorillonite stability, about 400°C and perhaps 450°C, respectively (Hemley and Jones, 1964, p. 564), or to areas at which solutions lead to other types of metasomatism. Other alteration zones similar to those associated with ore deposits may be present, especially at depth around conduits that lead to fumaroles. In general, these alteration assemblages range in the following sequence away from the conduit: advanced argillic (similar to the surficial zone here), sericitic, intermediate argillic, propylitic, and potassium silicic assemblages (Meyer and Hemley, 1967, p. 170).

REMOVAL OF ALTERED DEBRIS

HYPOTHETICAL SOURCES OF RAPID MASS MOVEMENTS

The alteration model of Sherman Crater may be expanded further to include hypothetical zones for rapid mass movement of debris (fig. 20). If alteration has occurred to the extent inferred in figure 19, avalanches from different areas or depths would contain material that had been altered to a different degree. Avalanches of outer rim material (above surface I, fig. 20) would involve some deposits that were hydrothermally altered prior to eruption (shb1) or that were highly

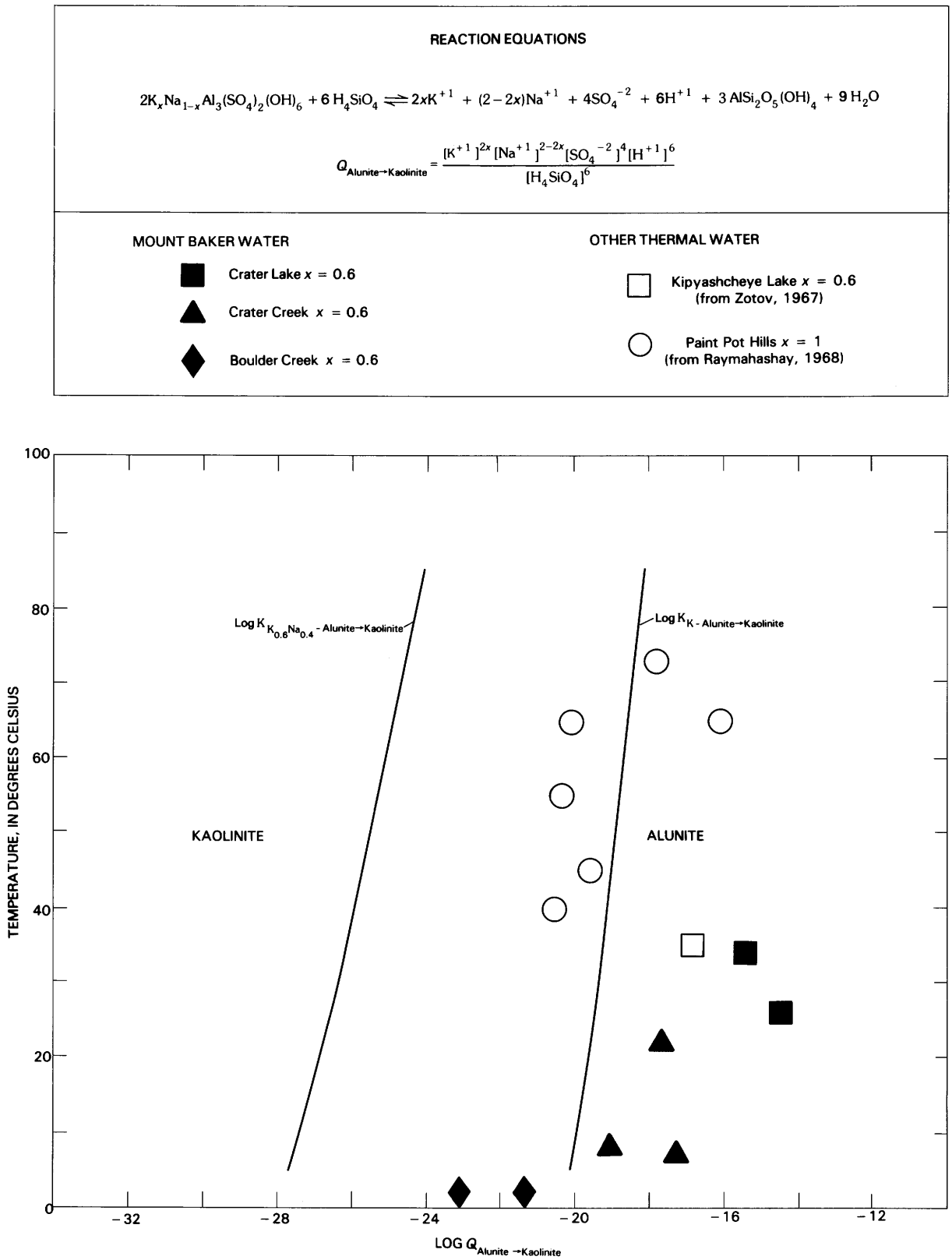

FIGURE 17.—Alunite-kaolinite stability in acid-sulfate waters. Entropy change (ΔS_r°) for the reaction is assumed to be constant with change in temperature and alunite species. Free energy at other than 25°C (298K) is approximated by $\Delta G_{r,T}^\circ = \Delta G_{r,298K}^\circ - \Delta S_{r,298K}^\circ (T-298K)$.

SULFUR OXIDATION NEAR THE GROUND SURFACE

$$H_2S + \tfrac{1}{2}O_2 \rightleftharpoons H_2O + S^\circ$$

$$S^\circ + O_2 \rightleftharpoons SO_2$$

$$SO_2 + \tfrac{1}{2}O_2 \rightleftharpoons SO_3$$

$$SO_3 + H_2O \rightleftharpoons H_2SO_4$$

FIGURE 18 (left).—Possible model of surficial, acid-alteration zone; modified from Schoen, White, and Hemley (1974, p. 4, fig. 10).

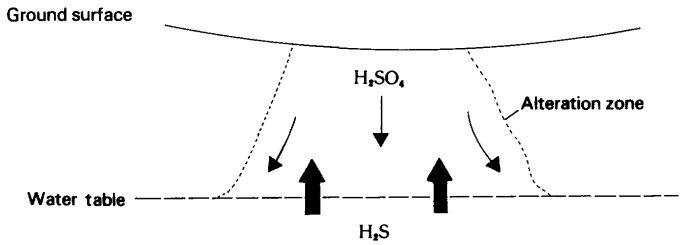

FIGURE 19 (below).—Inferred pattern of alteration zones in vent-filling debris in Sherman Crater. Hydrogen sulfide from fumarole conduits is oxidized to sulfuric acid, which then proceeds to alter surrounding rock by hydrogen metasomatism. The dominant, fine-grained alteration product in zones of decreasing intensity ranges from silica alone to alunite, kaolinite, and smectite. Line of section *C–C′* is shown on plate 1.

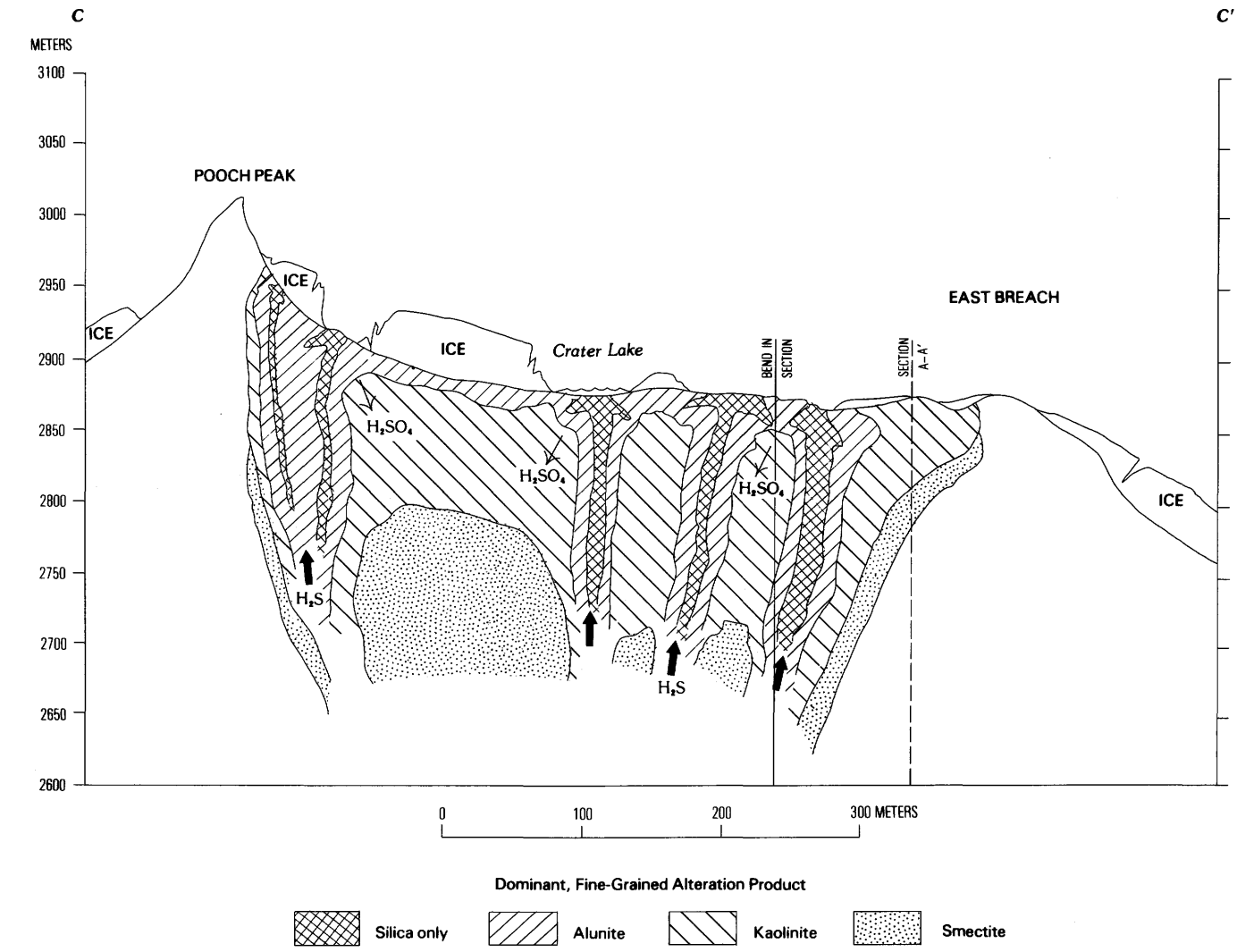

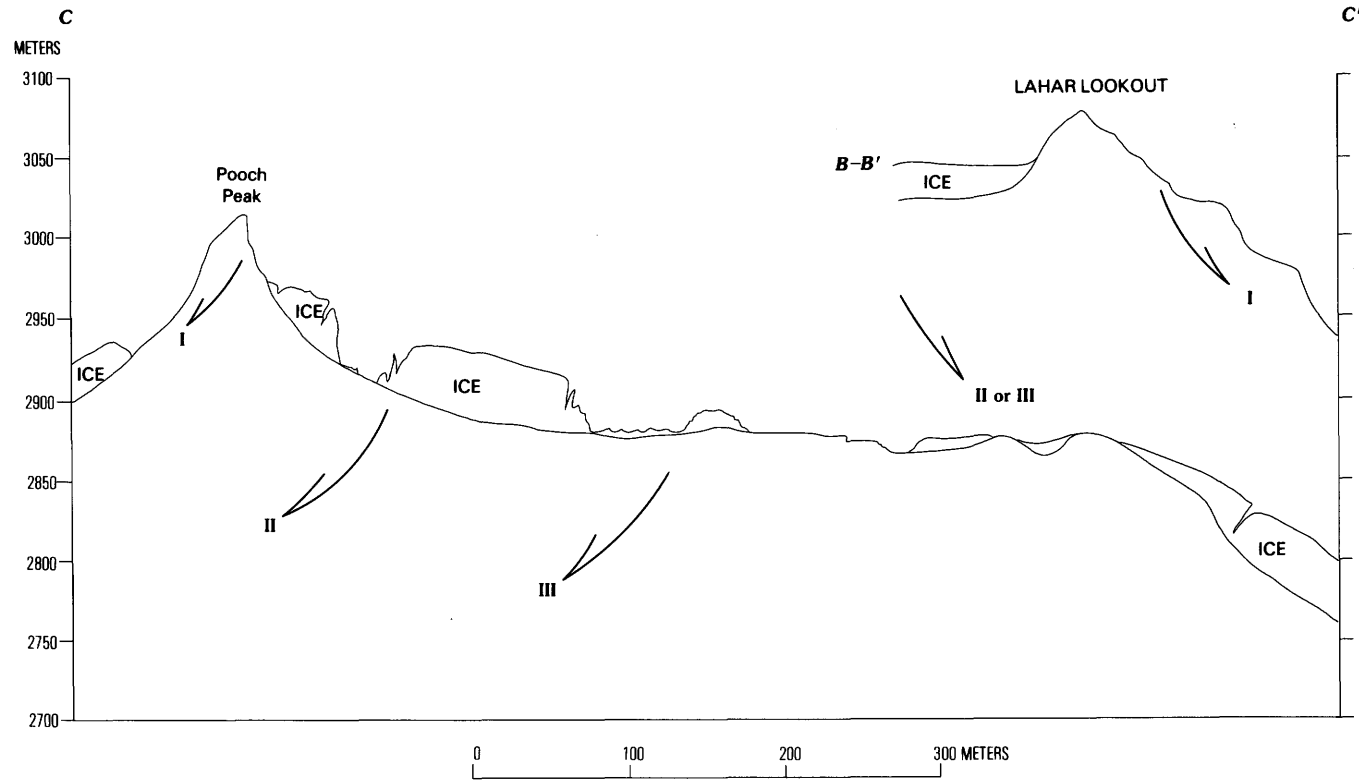

FIGURE 20.—Hypothetical slip surfaces for large mass movements. In comparison with figure 19, an avalanche above surface I would be expected to contain unaltered rock, weathered debris, and some material that could have been hydrothermally altered prior to eruption. An avalanche that included a large amount of the area of concentrated fumarolic activity, as above surface II, might contain a large amount of alunite. An avalanche that included debris from the central part of the vent, as above surface III, might contain a predominant amount of clay minerals, especially kaolinite. Lines of section *B–B'* and *C–C'* are shown on plate 1.

weathered (shb2) but the bulk of the avalanche debris would be relatively less altered than debris found within the crater. Avalanches of inner rim material (above surface II, fig. 20) would contain assemblages associated principally with fumarolic conduits, particularly rich in silica or alunite but probably having only a small or moderate amount of clay minerals. Avalanches derived from the main part of the vent-filling debris (above surface III, fig. 20) would contain an abundance and variety of clays.

Probably neither of the two young tephras (shb1 and shb2) at Sherman Crater represent the kind of deposit that could provide a source of large masses of kaolinite or alunite for avalanches from zones such as above surface I in figure 20. Unit shb2 contains little of these minerals and shb1, although rich in these minerals, is too thin a deposit to be a significant source. If the Holocene mudflows that contain abundant kaolinite or alunite originated from areas outside the crater rim, sources of altered tephra must have been thicker in those areas than the deposits recognized in this study. Such thick, altered tephras are not apparent on the lower slopes of the volcano and thus probably were not present on the crater rim. The clay- and alunite-rich mudflows, therefore, more likely came from other zones, such as above surfaces II or III in figure 20, possibly after much of a relatively unaltered rim had been removed by piecemeal erosion.

Of those mudflows that contain hydrothermally altered material, kaolinite is more abundant in the younger mudflows (samples B3, B4, P1) relative to the older mudflows (samples M2, P2), which indicates that the younger mudflows were initiated in relatively less leached but more clayey zones than the older mudflows. Therefore, the younger mudflows may have originated in areas closer to the core of the volcano, and the older mudflows, in zones near the fumarole vents but peripheral to the core. At present, the largest erosional inroad to the core of Sherman Crater is the east breach, which is the general source area of the two young, kaolinite-rich Boulder Creek mudflows (Samples B3, B4).

UNUSUALLY LARGE MASS MOVEMENTS

The Holocene history of rapid mass movements and the present topography and thermal activity at Mount Baker suggest that the largest avalanche or mudflow to descend the volcano in the future would most likely be 20–30 $\times$ 10^6 m^3 (Frank and others, 1977, p. 36). The

removal zones shown in figure 20 illustrate the type of source areas that could accommodate all the large mudflows that originated on the upper cone of Mount Baker during the last 10,000 years, as well as future avalanches or mudflows of as much as 30×10^6 m^3. Frank, Meier, and Swanson (1977, p. 36) believed that at present the most likely, though not only, source for such a future event is Lahar Lookout.

The distribution of hydrothermal clay at Sherman Crater suggests that even larger mass movements of clay-rich material might be possible from the upper cone. If, as in some geothermal areas elsewhere, significant amounts of clay minerals and other poorly consolidated alteration products occur as deep as 900 m below Sherman Crater, then about 0.2×10^9 m^3 of clay-rich material would directly underlie the crater. The structure of the upper part of Mount Baker could then be considered analogous to a chocolate-dipped ice cream cone; that is, a relatively low-strength interior of clayey debris sheathed by a more competent coating of less-altered, layered lavas and breccias. If the outer layers were ruptured, such as by steam explosion, ground-faulting, piecemeal erosion, or eruption, the interior could then readily provide material for unusually large mass movements.

Sudden removal of the upper half of a 900-m-thick cylinder or plug of clayey vent-filling debris plus a quadrant of the enclosing cone would yield a rock avalanche with an estimated volume of about 1×10^9 m^3 and a cirquelike amphitheater 1–2 km across. If all 900 m of altered material and an enclosing quadrant were removed, the avalanche volume would be about 3×10^9 m^3 and would produce an amphitheater 2–4 km across.

There is no evidence that such huge events occurred in the recent past at Mount Baker, but they have at Mount Rainier, Wash., another Cascade Range volcano of generally similar shape, structure, and petrology. The Electron Mudflow of about 0.2×10^9 m^3 occurred 600 years ago at Mount Rainier, and the Osceola Mudflow of about 2×10^9 m^3 occurred 5,700 years ago (Crandell, 1971, p. 24–26, 56–57). Both of these mudflows contain significant amounts of hydrothermally produced clay (Crandell, 1971, p. 28, 56), and they provide well-documented examples of the unusually large mass movements just described.

In view of the somewhat smaller size of Mount Baker, mass movements larger than a few hundred thousand cubic meters might not be as likely as at Mount Rainier. Nevertheless, a huge volume of poorly consolidated material possibly is present within Mount Baker. If such a mass exists, probably only some discrete violent event such as highly explosive eruption or a large-intensity earthquake could trigger its abrupt mobilization and rapid removal.

CONCLUSIONS

Sherman Crater and the Dorr Fumarole Field at Mount Baker contain extensive deposits of hydrothermal alteration products. Locally in both of these areas, hydrothermal alteration is currently taking place. Extensive hydrothermal alteration at Sherman Crater has also occurred at least as far back as 6,000 years ago as indicated by the distribution of hydrothermal products in deposits of Holocene mudflows that originated from the crater area. The large amount of clay-rich products, particularly kaolinite, in the younger deposits indicates that at Sherman Crater either progressive erosion has cut into more clayey parts of the core or that the amount of clayey material has increased through time. The distribution of kaolinite and the solution chemistry of surficial water suggest that kaolinite is formed principally at some depth below the surface of the crater. At the surface, the predominant fine-grained, crystalline alteration product is alunite.

ADDENDUM

After completion of the manuscript for this report, an unusually large debris avalanche occurred 280 km south of Mount Baker at Mount St. Helens volcano on May 18, 1980. Following 8 weeks of repeated earthquakes and relatively mild phreatic eruptions, a magnitude 5.1 earthquake triggered an avalanche of 2.5–3.0 km^3; the avalanche was followed by a laterally directed explosion and a magmatic eruption that continued for several hours (Lipman and Mullineaux, 1981). The amphitheater-shaped crater that resulted from these events was about 2 km wide, 4 km long, and 700 m deep. Subsequent studies by Pevear, Dethier, and Frank (1982) show that hydrothermally formed smectite was pervasive in old rock material from the inside of the cone, including the debris avalanche and the pre-May 18 lithic tephra. The large avalanche probably would not have occurred without the disruptive forces that accompanied the injection of new magma into the cone.

REFERENCES CITED

Babcock, J. W., and Wilcox, R. E., 1977, Results of petrographic examination of samples, *in* Assessment of increased thermal activity at Mount Baker, Washington, March 1975–March 1976: U.S. Geological Survey Professional Paper 1022–A, p. A25–A26.

Bockheim, J. G., 1972, Effects of alpine and subalpine vegetation on soil development, Mount Baker, Washington: Seattle, Wash., University of Washington Ph.D. thesis, 171 p.

Bockheim, J. G., and Ballard, T. M., 1975, Hydrothermal soils of the crater of Mount Baker, Washington: Soil Science Society of America, 1975, Proceedings, v. 39, no. 5, p. 997–1001.

Bortleson, G. C., Wilson, R. T., and Foxworthy, B. L., 1976, Water-quality effects on Baker Lake of recent volcanic activity at Mount Baker, Washington: U.S. Geological Survey Professional Paper 1022–B, 30 p.

Brophy, G. P., Scott, E. S., and Snellgrove, R. A., 1962, Sulfate studies—2, Solid solution between alunite and jarosite: American Mineralogist, v. 47, p. 112–126.

Brown, G., ed., 1961, The X-ray identification and crystal structure of clay minerals [2d ed.]: London, Mineralogical Society, 544 p.

Carroll, Dorothy, 1970, Clay minerals—A guide to their X-ray identification: Geological Society of America Special Paper 126, 80 p.

Coombs, H. A., 1939, Mt. Baker, a Cascade volcano: Geological Society of America Bulletin, v. 50, no. 10, p. 1493–1509.

Crandell, D. R., 1971, Postglacial lahars from Mount Rainier volcano, Washington: U.S. Geological Survey Professional Paper 677, 75 p.

Easterbrook, D. J., and Rahm, D. A., 1970, Landforms of Washington: Bellingham, Washington, Western Washington State College, 156 p.

Eichelberger, J. C., Heiken, Grant, Widdicombe, R., Wright, D., Keady, C. J., and Cobb, D. D., 1976, New fumarolic activity on Mt. Baker—Observations during April through July 1975: Journal of Volcanology and Geothermal Research, v. 1, no. 1, p. 35–53.

Frank, David, and Post, Austin, 1976, Documentation of thermal changes by photographs of snow and ice features at Mount Baker, Washington [abs.]: EOS (American Geophysical Union Transactions), v. 57, no. 2, p. 87.

Frank, David, Post, Austin, and Friedman, J. D., 1975, Recurrent geothermally induced debris avalanches on Boulder Glacier, Mount Baker, Washington: U.S. Geological Survey Journal of Research, v. 3, no. 1, p. 77–87.

Frank, David, Meier, M. F., and Swanson, D. A., 1977, Assessment of increased thermal activity at Mount Baker, Washington, March 1975–March 1976: U.S. Geological Survey Professional Paper 1022-A, 49 p.

Friedman, J. D., and Frank, David, 1980, Infrared surveys, radiant flux, and total heat discharge at Mount Baker volcano, Washington, between 1970 and 1975: U.S. Geological Survey Professional Paper 1022-D, 33 p.

Garrels, R. M., and Christ, C. L., 1965, Solutions, minerals, and equilibria: New York, Harper and Row, 450 p.

Hem, J. D., 1968, Graphical methods for studies of aqueous aluminum hydroxide, fluoride, and sulfate complexes: U.S. Geological Survey Water-Supply Paper 1827-B, 33 p.

Hemley, J. J., and Jones, W. R., 1964, Chemical aspects of hydrothermal alteration with emphasis on hydrogen metasomatism: Economic Geology, v. 59, p. 538–567.

Hendricks, S. B., 1937, The crystal structure of alunite and the jarosites: American Mineralogist, v. 22, no. 6, p. 773–784.

Hyde, J. H., and Crandell, D. R., 1978, Postglacial volcanic deposits at Mount Baker, Washington, and potential hazards from future eruptions: U.S. Geological Survey Professional Paper 1022-C, 17 p.

Iwao, Shuichi, 1968, Zonal structure in some kaolin and associated deposits of hydrothermal origin in Japan: International Geological Congress, 23d, Prague, 1968, Proceedings, v. 14, p. 107–113.

Jones, J. B., and Segnit, E. R., 1971, The nature of opal; I, Nomenclature and constituent phases: Geological Society of Australia Journal, v. 18, pt.1, p. 57–67.

Kittrick, J. A., and Hope, E. W., 1963, A procedure for the particle-size separation of soils for X-ray diffraction analysis: Soil Science, v. 96, p. 319–325.

Krimmel, R. M., and Frank, David, 1980, Aerial observations of Mount Baker, Washington—1976–1979 update [abs.]: EOS (American Geophysical Union Transactions), v. 81, no. 6, p. 69.

Lipman, P. W., and Mullineaux, D. R., 1981, The 1980 eruptions of Mount St. Helens, Washington: U.S. Geological Survey Professional Paper 1250, 844 p.

Malone, S. D., 1979, Gravity changes accompanying increased heat emission at Mount Baker, Washington: Journal of Volcanology and Geothermal Research, v. 6, p. 241–256.

Malone, S. D., and Frank, David, 1975, Increased heat emission from Mount Baker, Washington: EOS (American Geophysical Union Transactions), v. 56, no. 10, p. 679–685.

Meyer, C., and Hemley, J. J., 1967, Wall rock alteration, *in* H. L. Barnes, ed., Geochemistry of hydrothermal ore deposits: New York, Holt, Rinehart, and Winston, Inc., p. 166–235.

Millot, Georges, 1970, Geology of clays—Weathering, sedimentology, geochemistry [translated from French by W. R. Farrand and Hélène Paquet]: New York, Berlin, Springer-Verlag, 429 p.

Mullineaux, D. R., 1974, Pumice and other pyroclastic deposits in Mount Rainier National Park, Washington: U.S. Geological Survey Bulletin 1326, 83 p.

Narebski, Wojciech, and Paulo, Andrzej, 1973, Solfataric alteration products of andesitic lavas in the crater of Cotopaxi volcano, Ecuador: Mineralogia Polonica, v. 4, p. 67–80.

Parker, R. L., 1962, Isomorphous substitution in natural and synthetic alunite: American Mineralogist, v. 47, p. 127–136.

Pevear, D. R., Dethier, D. P., and Frank, David, 1982, Clay minerals in the 1980 deposits from Mount St. Helens: Clays and Clay Minerals, v. 30, no. 4, p. 241–252.

Raymahashay, B. C., 1968, A geochemical study of rock alteration by hot springs in the Paint Pot Hill area, Yellowstone Park: Geochimica et Cosmochimica Acta, v. 32, p. 499–522.

Reynolds, R. C., Jr., 1971, Clay mineral formation in an alpine environment: Clays and Clay Minerals, v. 19, p. 361–374.

Robie, R. A., Hemingway, B. S., and Fisher, J. R., 1978, Thermodynamic properties of minerals and related substances at 298.15 K and 1 bar (10^5 pascals) pressure and at higher temperatures: U.S. Geological Survey Bulletin 1452, 456 p.

Schoen, Robert, White, D. E., and Hemley, J. J., 1974, Argillization by descending acid at Steamboat Springs, Nevada: Clays and Clay Minerals, v. 22, p. 1–22.

Slansky, Ervin, 1973, The thermal investigation of alunite and natroalunite: Neues Jahrbuch für Mineralogie Monatshefte, v. 1973, no. 3, p. 124–138.

_____1975, Natroalunite and alunite from White Island volcano, Bay of Plenty, New Zealand: New Zealand Journal of Geology and Geophysics, v. 18, no. 2, p. 285– 293.

Steiner, A., 1953, Hydrothermal rock alteration at Wairakei, New Zealand: Economic Geology, v. 48, no. 1, p. 1–13.

_____1968, Clay minerals in hydrothermally altered rocks at Wairakei, New Zealand: Clays and Clay Minerals, v. 16, p. 193–213.

Sumi, Kiyoshi, 1970, Zonal distribution of clay minerals in the Matsukawa geothermal area, Japan: International Clay Conference, Tokyo, 1970, Proceedings, v. 1, p. 501–512.

Swan, V. L., 1978, Mount Baker volcanics: Pacific Northwest regional meeting of American Geophysical Union, 25th, Portland, 1978, Proceedings, p. 42–46.

Yamasaki, T., Matsumoto, Y., and Hayashi, M., 1970, The geology and hydrothermal alterations of Otake geothermal area, Kujyo volcano group, Kyushu, Japan: Geothermics, special issue 2, v. 2, pt. 1, p. 197–207.

Zotov, A. V., 1967, Recent formation of alunite in the Kipyashcheye ("Boiling") Crater Lake, Golovnin volcano, Kunashir Island: Akademiya Nauk Armyanskoy SSR Doklady, v. 174, p. 124–127.